Spatial distribution of selenium-mercury in Arctic seabirds

Marta Cruz-Flores, Jérémy Lemaire, Maud Brault-Favrou, Signe Christensen-Dalsgaard, Carine Churlaud, Sébastien Descamps, Kyle Elliott, Kjell Einar Erikstad, Alexey Ezhov, Maria Gavrilo, et al.

Spatial distribution of selenium-mercury in Arctic seabirds

Marta Cruz-Flores [a,*], Jérémy Lemaire [a,b], Maud Brault-Favrou [a], Signe Christensen-Dalsgaard [c], Carine Churlaud [a], Sébastien Descamps [d], Kyle Elliott [e], Kjell Einar Erikstad [f], Alexey Ezhov [g], Maria Gavrilo [h], David Grémillet [i,j], Gaël Guillou [a], Scott Hatch [k], Nicholas Per Huffeldt [l,p], Alexander S. Kitaysky [m], Yann Kolbeinsson [n], Yuri Krasnov [g], Magdalene Langset [c], Sarah Leclaire [o], Jannie F. Linnebjerg [p], Erlend Lorentzen [d], Mark L. Mallory [q], Flemming R. Merkel [l,p], William Montevecchi [r], Anders Mosbech [p], Allison Patterson [e], Samuel Perret [i], Jennifer F. Provencher [s], Tone K. Reiertsen [f], Heather Renner [t], Hallvard Strøm [d], Akinori Takahashi [u], Jean-Baptiste Thiebot [u,v], Thorkell Lindberg Thórarinsson [n], Alexis Will [m,w], Paco Bustamante [a], Jérôme Fort [a]

[a] *Littoral, Environnement et Sociétés (LIENSs), UMR 7266 CNRS – La Rochelle Université, 2 rue Olympe de Gouges, 17000 La Rochelle, France*

[b] *Department of Behavioral and Cognitive Biology, University of Vienna, Djerassiplatz 1, 1030 Vienna, Austria*

[c] *Norwegian Institute for Nature Research. 7485 Trondheim, Norway*

[d] *Norwegian Polar Institute, Fram Centre. 9296 Tromsø, Norway*

[e] *Department of Natural Resource Sciences, McGill University. Ste Anne-de-Bellevue, Quebec, Canada H9X 3V9*

[f] *Norwegian Institute for Nature Research, FRAM Centre. 9296 Tromsø, Norway*

[g] *Murmansk Marine Biological Institute Russian Academy of Science, 183010 Vladimirskaya Str. 17, Murmansk, Russia*

[h] *Arctic and Antarctic Research Institute. 199397 St. Petersburg, Russia*

[i] *CEFE, Univ Montpellier, CNRS, EPHE, IRD, Montpellier, France*

[j] *Percy FitzPatrick Institute of African Ornithology, University of Cape Town, Rondebosch, South Africa*

[k] *U.S. Geological Survey, Alaska Science Center. Anchorage, AK 99508, USA*

[l] *Greenland Institute of Natural Resources, 3900 Nuuk, Greenland*

[m] *University of Alaska Fairbanks, Institute of Arctic Biology, Department of Biology & Wildlife. Fairbanks, AK 99775-7000, USA*

[n] *Northeast Iceland Nature Research Centre. 640 Húsavík, Iceland*

[o] *Laboratoire Evolution et Diversité Biologique (EDB), UMR 5174, Université de Toulouse, CNRS, IRD. 31062 Toulouse, France*

[p] *Department of Ecoscience, Aarhus University. 4000 Roskilde, Denmark*

[q] *Biology, Acadia University, Wolfville, Nova Scotia B4P 2R6, Canada*

[r] *Memorial University of Newfoundland and Labrador. St. John's, Newfoundland A1C 3X9, Canada*

[s] *Ecotoxicology and Wildlife Health Division, Environment and Climate Change Canada, Ottawa, Ontario, Canada, K1A 0H3*

[t] *U.S. Fish and Wildlife Service, Alaska Maritime Wildlife Refuge, Homer, AK, USA*

[u] *National Institute of Polar Research, 10-3 Midori-cho, Tachikawa. Tokyo 190-8518, Japan*

[v] *Graduate School of Fisheries Sciences, Hokkaido University, 3-1-1 Minato-cho, Hakodate, Hokkaido 041-8611, Japan*

[w] *World Wildlife Fund, US Arctic Program, 810 N Street, Suite 300, Anchorage AK 99501, USA*

* Correspondence: Marta Cruz-Flores, Littoral, Environnement et Sociétés, UMR 7266 CNRS – La Rochelle Université, 2 Rue Olympe de Gouges, 17000 La Rochelle, France

Email: martacruzflores@gmail.com

Running title: Se and Hg spatial distribution in Arctic seabirds

ABSTRACT

Mercury (Hg) is a metallic trace element toxic for humans and wildlife that can originate from natural and anthropic sources. Hg spatial gradients have been found in seabirds from the Arctic and other oceans, suggesting contrasting toxicity risks across regions. Selenium (Se) plays a protective role against Hg toxicity, but its spatial distribution has been much less investigated than that of Hg. Between 2015-2017, we measured spatial co-exposure of Hg and Se in blood samples of two seabird species, the Brünnich's guillemot (*Uria lomvia*) and the black-legged kittiwake (*Rissa tridactyla*) from 17 colonies in the Arctic and subarctic regions, and we calculated their molar ratios (Se:Hg), as a measure of Hg sequestration by Se and, therefore, of Hg exposure risk. We also evaluated concentration differences between species and ocean basins (Pacific-Arctic and Atlantic-Arctic), and examined the influence of trophic ecology on Hg and Se concentrations using nitrogen and carbon stable isotopes. In the Atlantic-Arctic ocean, we found a negative west-to-east gradient of Hg and Se for guillemots, and a positive west-to-east gradient of Se for kittiwakes, suggesting that these species are better protected from Hg toxicity in the European Arctic. Differences in Se gradients between species suggest that they do not follow environmental Se spatial variations. This, together with the absence of a general pattern for isotopes influence on trace element concentrations, could be due to foraging ecology differences between species. In both oceans, both species showed similar Hg concentrations, but guillemots showed lower Se concentrations and Se:Hg than kittiwakes, suggesting a higher Hg toxicity risk in guillemots. Within species, neither Hg, nor Se or Se:Hg differed between both oceans. Our study highlights the importance of considering Se together with Hg, along with different species and regions, when evaluating Hg toxic effects in marine predators in international monitoring programs.

KEYWORDS: Toxics, Atlantic-Arctic, Pacific-Arctic, blood, stable isotopes, black-legged kittiwake, Brünnich's guillemot, thick-billed murre

INTRODUCTION

Mercury (Hg) is a widespread toxic pollutant of major concern, that can cause severe health damage in both humans and wildlife, even at low concentrations (Wolfe et al. 1998; Tan et al. 2009). Although Hg can originate from natural sources, human activities such as mining or fossil fuel combustion, have resulted in an increase in Hg concentrations in the environment since the industrial revolution (Sen and Peucker-Ehrenbrink 2012). Once in the environment, Hg is methylated by microorganisms producing the most toxic and bioavailable form of Hg, methyl-Hg (MeHg). MeHg is bioaccumulated within marine organisms (i.e., its concentrations increase within the body over time) and biomagnified through marine food webs (i.e., its concentrations increase along the trophic chain; Bargagli et al. 1998; Seco et al. 2021). Hence, long-lived meso or top predators such as marine mammals and seabirds are among the most contaminated species and they are, thus, vulnerable to Hg toxicity. For instance, ecophysiological impacts due to MeHg toxicity have been found in birds with blood-equivalent Hg concentrations above 1 μg. g^{-1} wet weight (ww; Ackerman et al. 2016). In response to these concerns, large international programs and monitoring assessments have been created to further understand Hg contamination and its impacts on marine predators and to monitor its spatial variations at a large scale (e.g., UN Environment 2019).

Selenium (Se) is an essential element that naturally occurs in the environment and can also be released into the atmosphere by human activities (Mehdi et al. 2013). Animals acquire Se through their diet, and its concentration must be considered along with Hg when evaluating Hg effects and toxicity risks to wildlife. Indeed, Se is known to protect organisms from Hg toxicity (Cuvin-Aralar and Furness 1991). For instance, in the (sub)Antarctic regions, skua populations with high Hg concentrations but also high Se:Hg molar ratios (hereafter Se:Hg) showed limited Hg effects on population growth, while populations with low Hg but three times lower Se:Hg than the previous ones showed negative effects in their reproduction (Goutte et al. 2014b; Carravieri et al. 2017). That produced a strong impact on their population growth, suggesting important Hg toxic effects (Goutte et al. 2014b; Carravieri et al. 2017). These results were due to the MeHg affinity for Se, which is depleted, and its selenoenzymes inhibited, ultimately producing Hg toxicity effects due to Se deficiency together with MeHg toxicity (Ralston and

Raymond 2018). These effects become increasingly apparent as MeHg concentrations approach, and especially exceed, equimolar stoichiometries with Se. Moreover, MeHg can be detoxified as insoluble mercury selenide (HgSe) in birds (Nigro and Leonzio 1996; Manceau et al. 2021). However, this detoxification capacity depends on the available Se and its speciation, as the intermediate compound in the demethylation reaction involves a selenocysteinate complex ($Hg(Sec)_4$), which presents a Se:Hg of 4:1. Thus, demethylation can severely deplete the stock of bioavailable Se for other biological functions (Manceau et al. 2021). Therefore, Se:Hg is considered to reflect Hg sequestration and Se depletion, and is widely used to assess Hg exposure risk. Nevertheless, only a few studies have quantified Hg-Se co-exposure and interaction in seabirds and other marine predators (González-Solís et al. 2002; Carvalho et al. 2013; Cipro et al. 2014; Øverjordet et al. 2015a) and none have considered its large-scale spatial variations.

In the Arctic and subarctic regions, high Hg levels have been found in seabirds, and their effects on their reproduction, behaviour, survival, and population dynamics have been pointed out (AMAP 2011; Chastel et al. 2022). In addition, previous investigations demonstrated a strong spatial variability in seabird Hg contamination across the Arctic and subarctic regions, suggesting contrasting associated risks for populations according to specific areas (Renedo et al. 2020; Albert et al. 2021). However, to the best of our knowledge, no study previously investigated the spatial variation in Se in the Arctic. This is nonetheless essential to fully grasp the potential risk associated with Hg in Arctic marine biota.

In this study, we analysed blood Hg and Se concentrations in two seabird species, the Brünnich's guillemot or thick-billed murre *Uria lomvia* (hereafter guillemots) and the black-legged kittiwake *Rissa tridactyla* (hereafter kittiwakes) from 17 colonies distributed within the Arctic and subarctic regions. Our objectives were (i) to provide the first information about Se spatial variability in marine predators, (ii) to evaluate if the predicted spatial variability in Hg toxicity risk could change when considering the spatial variability of Se; and (iii) to evaluate if Hg and Se concentrations, and their spatial distribution, are different between species due to their dissimilar trophic ecologies, since guillemots present generally a diving foraging behaviour in continental-shelf and continental-slope waters and are considered less

generalist than kittiwakes, which present an opportunistic pelagic surface-foraging behaviour (Gaston and Hipfner 2020; Hatch et al. 2020). To do so, we analysed nitrogen and carbon stable isotopes, as proxies of bird trophic position ($\delta^{15}N$) and feeding habitat ($\delta^{13}C$; Newsome et al. 2007).

We made the following a priori predictions: (i) Hg concentrations will increase from east to west for Atlantic-Arctic kittiwake populations, as has previously been shown in auks including guillemots by Albert et al. (2021), but we did not make predictions for the spatial variation of Se due to the scarce knowledge on this element in the marine environment (Cutter and Bruland 1984); (ii) Hg and Se concentrations and their spatial variation are influenced by differences in the birds' trophic position, reflected in their $\delta^{15}N$ and $\delta^{13}C$ ratios; (iii) Se:Hg differs between species due to their different foraging ecologies, with guillemots showing lower Hg concentrations than kittiwakes, as already described by (Chastel et al. 2022), and lower Se concentrations due their more coastal behaviour (higher $\delta^{13}C$ values) than kittiwakes, as found for other inshore top predators (AMAP 2018; Carravieri et al. 2020; Damseaux et al. 2021).

METHODOLOGY

Populations of study

Fieldwork was conducted between 2015 and 2017 at 17 different colony sites (Fig. 1), all of them located in the Arctic and subarctic regions. Details on colony sites, specific sampling years for each colony, and sampling sizes are provided in Table 1.

Blood samples (0.5 ml) were collected from adult breeding birds from the brachial vein from early to mid-chick rearing period, allowing inter-species and inter-population comparisons. Blood samples were stored in 70% ethanol until analyses when they were freeze-dried for 48 hrs, grounded, and homogenized. In total, 65 guillemots and 64 kittiwakes were sampled (Table 1).

Trace elements and isotopic analyses

All analyses were performed on dry whole blood at the Littoral Environnement et Sociétés (LIENSs), La Rochelle, France. Hg and Se concentrations in whole blood samples are assumed to reflect the exposure of the Hg and Se ingested for a period of up to 2 months (Monteiro and Furness 2001) due to blood turnover. Thus, in the case of this study, whole blood samples would reflect the period when birds were at or near the breeding site. Isotopic values in whole blood samples reflect bird foraging ecology one or two months prior to the sampling (Buchheister and Latour 2010).

Total Hg (hereafter Hg) concentrations were determined by direct measurement using an atomic absorption spectrometer AMA-254 (Advanced Mercury Analyser-254; Altec®). Two replicates of 1 - 2 mg dry weight (dw) were analysed for each sample. The reproducibility of duplicate samples was approved when the Relative Standard Deviation (RSD) was < 10%. If the RSD was > 10%, then a third sample was analysed. We used the mean value of the two measurements with RSD < 10% for subsequent statistical analyses. For validation of the method, the analyses of Certified Reference Material (CRM) TORT-2 (lobster hepatopancreas from the National Research Council of Canada, NRCC) were performed at the beginning and at the end of the analytical cycle and every 10 samples. TORT-2 certified Hg concentration is (mean ± SD) 0.27 ± 0.06 $\mu g.g^{-1}$ dw, and measured value was 0.26 ± 0.00 µg.g-1 dw, giving a recovery of 95.99 ± 1.63 % (n=13). Blanks were also performed at the beginning of each measurement session. The limit of quantification of the AMA was 0.05 ng, and the detection limit was 0.01 ng. Hg concentrations are presented in $\mu g.g^{-1}$ dw.

Prior to Se quantification, between 0.10 - 0.24 g of dry blood was acid-digested in a mixture of 6 mL of 70% HNO_3 (VWR Quality SUPRAPUR) and 2 mL of 30% HCl (VWR Quality SUPRAPUR). Acid digestion was performed overnight under ambient temperature and then heated in a microwave during 30 min with increasing temperature until 105°C, and 15 min at 105°C (1200 W) using a Milestone Start-D microwave and polypropylene conical bottom centrifuge tubes to do the mineralization. For samples weighing less than 0.10 g, the volumes of HNO_3 and HCl were divided by two. Samples were further diluted with ultrapure water to 50 mL (25 mL for samples < 0.10 g). To avoid contamination, analysis

and preparation of samples and standards were carried out in a clean room. In addition, all utensils used were soaked in a bath of diluted 5% HNO_3 (VWR Quality NORMAPUR) for at least 48 h, rinsed in ultrapure water and dried. Se quantification was performed by Inductively Coupled Plasma (ICP) Mass Spectrometry (ICP-MS II Series Thermo Fisher Scientific). CRMs DOLT-5 (dogfish liver, NRCC), and TORT-3 (lobster hepatopancreas, NRCC), were treated and analysed as samples. Three replicates were analysed for each sample and the mean value was used in statistical analyses. Results of CRMs for Se displayed recoveries of 107.40 ± 0.08 % for DOLT-5, and 112.60 ± 16.04 % for TORT-3. The limit of quantification of the IPC was 2 $\mu g.l^{-1}$, and the detection limit was 0.20 $\mu g.l^{-1}$. Se concentrations are presented in $\mu g.g^{-1}$ dw.

Carbon and nitrogen stable isotope analyses were performed using a continuous-flow isotope-ratio mass spectrometer (Delta V Plus, Thermo Scientific) with a Conflo IV interface coupled to an elemental analyser (Flash 2000, Thermo Scientific). The $\delta^{15}N$ and $\delta^{13}C$ values are expressed in δ notation as deviations from standards (N_2 in air for $\delta^{15}N$, and Vienna Pee Dee Belemnite for $\delta^{13}C$), in ‰, according to the formula:

$$\delta X = \left[\left(\frac{\text{Rsample}}{\text{Rstandard}}\right) - 1\right] \times 1000$$

where X is ^{15}N or ^{13}C, R_{sample} is the isotopic ratio of the sample and $R_{standard}$ is the isotopic ratio of the standard. Calibration was carried out using reference materials: USGS-61, USGS-63, IAEA-N_2, IAEA–NO_3, IAEA-600 for nitrogen; and USGS-24, USGS-61, USGS-63, IAEA-CH_6, IAEA-600 for carbon. The analytical precision of the measurements was <0.10 ‰ for carbon and nitrogen based on analyses of USGS-61 and USGS-63 used as laboratory internal standards.

Statistical analysis

We have considered the detoxification process of Hg by calculating Se:Hg using the following equation:

$$\text{Se: Hg} = \frac{\text{Se } (\mu g\ g^{-1}\ dw) * 78.96\ (g\ mol^{-1})}{\text{Hg } (\mu g\ g^{-1}\ dw) * 200.59\ (g\ mol^{-1})}$$

where 78.96 $g.mol^{-1}$ and 200.59 $g.mol^{-1}$ are the atomic mass of Se and Hg, respectively.

All data analyses were performed using Software R-4.1.1(R Core Team 2021). First, due to differences in the strong baseline isotopic values between the Atlantic-Arctic and the Pacific-Arctic regions (McMahon et al. 2013; Espinasse et al. 2020; Smith et al. 2021), colonies were split into two oceanic basins: the Atlantic-Arctic (15 colonies) and the Pacific-Arctic (2 colonies). Further, only Atlantic-Arctic colonies were investigated for spatial variations in trace elements and their relationship with trophic ecology. To do so, we carried out linear mixed models using the `lmer` function of the `lme4` package (Bates et al. 2015). Due to the heterogeneity between both species, we performed models separately for each one. We included Hg, Se and Se:Hg as response variables; longitude, latitude, $\delta^{15}N$ and $\delta^{13}C$ as explanatory variables (covariates), and colony and year as random factors to account for the lack of independence among samples from the same colony and/or year. In addition, based on visual exploration of the data, we also included the quadratic relationship of $\delta^{15}N$ and $\delta^{13}C$. Residuals of the models were inspected following Zuur et al. (2009). Within each set of nested models per trace element and species, we performed model selection based on the Akaike Information Criterion corrected for small sample sizes (AICc) and we calculated the difference in AICc between each model and the model with the lowest AICc of each set (ΔAICc). We considered as good models those with an AICc lower than the null model and with an ΔAICc lower than 2, and we checked if the 95% CI of their factor effects overlapped with zero. We considered that a factor had a moderate effect when the overlap with zero was lower than 10%. We also calculated the weight of each model (Burnham and Anderson 2002).

Second, we compared Hg and Se concentrations, and Se:Hg (i) between species per ocean basin (Atlantic-Arctic and Pacific-Arctic), and (ii) within species between ocean basins. To do so, we performed linear mixed models including colony and year as a random factor, except for the differences between species in the Pacific-Arctic where we only had data for 2016.

Third, for each trace element and isotope, we calculated their mean and standard deviation per species and colony, and we evaluated if the differences between species within each colony were significant using Mann-Whitney U tests, as we had small sample sizes per colony and only one year of data per colony (except for the Kippaku colony).

Lastly, we explored biplots for $\delta^{15}N$ and $\delta^{13}C$ differentiated firstly by species, and secondly by species and colony. In order to evaluate the isotopic niche overlap between both species, and among species per colony, we carried out and plotted Standard Bayesian Ellipses (i) by species and (ii) by species and colony using the `createSiberObject` function from the `SIBER` package in R (Jackson et al. 2011). Finally, we calculated the Standard Ellipse Area (SEA) for both species and the overlap between them using the maximum likelihood estimates for means and covariance matrices for each group (i.e., species), using the `maxLikOverlap` function from the `SIBER` package.

RESULTS

Hg and Se spatial variations and influence of foraging ecology

In guillemots, we found strong support for a negative linear effect of longitude and a positive quadratic effect of $\delta^{13}C$ on Hg concentrations. In addition, we found moderate support for a positive linear effect $\delta^{15}N$ on guillemots Hg concentrations (Table 2). In kittiwakes, we found a strong support for a negative quadratic effect of $\delta^{15}N$, and a moderate support for a positive linear effect of $\delta^{13}C$ on Hg concentrations, but we did not find an effect of longitude. About Se concentrations, we found a moderate negative linear effect of longitude and a moderate negative linear effect of the interaction between longitude and $\delta^{15}N$ (Long: $\delta^{15}N$) in guillemots. In kittiwakes, we found strong support for a negative quadratic effect of $\delta^{15}N$ on Se concentrations, as well as moderate support for a positive linear effect of longitude and a positive linear effect of $\delta^{13}C$ on Se concentrations. Finally, for guillemots, we found strong support of a negative linear effect of $\delta^{15}N$ on Se:Hg ratios, and an absence of an effect of longitude. For kittiwakes, we did not find neither strong nor moderate effect of longitude or isotopes in Se:Hg ratios. The resulting regression functions are shown in Table 2. In all models the random factor colony explained a big part of the data variability.

Inter-specific and ocean basin differences in Hg and Se concentrations

Hg concentrations were similar between species in the Atlantic-Arctic (mean estimated from the model ± SE for guillemots: 1.07 ± 0.11 µg.g^{-1} dw; kittiwakes: 1.09 ± 0.12 µg.g^{-1} dw; $F_{1,111} = 0.01$; *p*-value = 0.90) and in the Pacific-Arctic (guillemots: 1.25 ± 0.25 µg.g^{-1} dw; kittiwakes: 1.08 ± 0.20 µg.g^{-1} dw; $F_{1,11.19} = 0.42$; *p*-value = 0.53; Figure 2). However, Se concentrations were significantly different between species in both oceans, with guillemots showing a mean Se concentration four times lower than black-legged kittiwakes in the Atlantic-Arctic (guillemots: 25.55 ± 5.10 µg.g^{-1} dw; kittiwakes: 97.16 ± 6.20 µg.g^{-1} dw; $F_{1,34.77} = 197.91$; *p*-value < 0.001) and three times lower in the Pacific-Arctic (guillemots: 22.72 ± 8.10 µg.g^{-1} dw; kittiwakes: 75.71 ± 5.02 µg.g^{-1} dw; $F_{1,11} = 42.82$; *p*-value < 0.001; Figure 2). Similarly, mean Se:Hg was three times lower for guillemots than for kittiwakes in both oceans, the Atlantic-Arctic (guillemots: 86.41 ± 16.89; kittiwakes: 261.36 ± 17.97; $F_{1,109.89} = 107.28$; *p*-value < 0.001) and the Pacific-Arctic (guillemots: 51.73 ± 23.50; kittiwakes: 165.85 ± 14.57; $F_{1,11} = 23.58$; *p*-value < 0.001; Figure 2).

Between the Atlantic-Arctic versus the Pacific-Arctic regions, guillemots showed no significant differences in Hg concentrations (mean estimated from the model ± SE for the Atlantic-Arctic: 1.27 ± 0.44 µg.g^{-1} dw; Pacific-Arctic: 1.50 ± 0.57 µg.g^{-1}; $F_{1,10.09} = 0.16$, *p*-value = 0.70) nor in Se concentrations (Atlantic-Arctic: 25.47 ± 6.41 µg.g^{-1}; Pacific-Arctic: 28.03 ± 8.46 µg.g^{-1}; $F_{1,10.09} = 0.09$; *p*-value = 0.77) or Se:Hg (Atlantic-Arctic: 79.35 ± 16.55; Pacific-Arctic: 51.73 ± 59.68; $F_{1,11} = 0.21$; *p*-value = 0.65). Similarly, in kittiwakes, neither Hg concentrations (Atlantic-Arctic: 0.99 ± 0.09 µg.g^{-1}; Pacific-Arctic: 1.08 ± 0.23 µg.g^{-1}; $F_{1,11.52} = 0.16$; *p*-value = 0.70) nor Se concentrations (Atlantic-Arctic: 95.39 ± 11.99 µg.g^{-1}; Pacific-Arctic: 71.72 ± 25.81 µg.g^{-1}; $F_{1,10.63} = 0.84$; *p*-value = 0.38), nor Se:Hg (Atlantic-Arctic: 268.01 ± 24.48; Pacific-Arctic: 168.23 ± 63.97; $F_{1,11.71} = 2.43$; *p*-value = 0.15) differed significantly between ocean basins.

Inter-colony differences in Hg and Se concentrations

Mean values per trace element and stable isotope per species and colony are shown in Table 1. In Alkefjellet (north of Spitsbergen, Svalbard archipelago, Norway, Atlantic-Arctic ocean) and the islet of

Bjørnøya (south of the Svalbard archipelago), guillemots had significantly lower Hg and Se concentrations than kittiwakes, but differences in Se:Hg were not significant (Table 1). In Isfjorden (mid-west of Spitsbergen), apart from significant differences in Hg and Se concentrations, there were also significant differences between species in Se:Hg, with lower values for guillemots than for kittiwakes. At Saint Lawrence Island (west coast of Alaska, USA, Pacific-Arctic ocean), Kippaku (mid-west coast of Greenland, Atlantic-Arctic ocean), Langanes (north-east of Iceland, Atlantic-Arctic ocean), Hornøya (north-east of Norway, Atlantic-Arctic ocean) and Cape Flora (south-west of the Franz Josef Archipelago, north of Russia, Atlantic-Arctic ocean) we did not measure significant differences in Hg concentrations between species, but there were significant differences in Se concentrations and, therefore, in Se:Hg, with lower values for guillemots than for kittiwakes. Nevertheless, birds from Thule (north-west of Greenland) showed a different pattern, with similar Se concentrations between species, but significantly higher Hg concentrations in guillemots than in kittiwakes. This implied a significant difference in Se:Hg at Thule, with guillemots showing lower values than kittiwakes (Table 1).

Inter-colony differences in isotopic ratios and niches

Thule was the only colony with significant differences in $\delta^{15}N$ values between species, with guillemots showing higher $\delta^{15}N$ values than kittiwakes (p-value < 0.05). In the case of $\delta^{13}C$ values, we found two colonies with significant differences between species: Saint Lawrence, where guillemots showed higher $\delta^{13}C$ values than kittiwakes (p-value < 0.05); and Cape Flora, where guillemots showed lower $\delta^{13}C$ values than kittiwakes (p-value < 0.01).

Standard Ellipses Areas were 3.0 and 2.9 units for guillemots and kittiwakes, respectively. The overlapping area between both was 2.2 units, and it comprised 74.7 and 77.2% of guillemots and kittiwakes' ellipses, respectively (Figure S1 in Supplementary Materials). At the colony level, only birds from Saint Lawrence Island in the Pacific-Arctic showed a clearly different isotopic niche compared to other colonies for both species (i.e., no overlap with other ellipses; Figure S2 in Supplementary Materials).

DISCUSSION

To our knowledge, this study is the first to simultaneously investigate the spatial distribution of Hg and Se concentrations in Arctic marine predators at a large spatial scale. We found differences in the longitudinal pattern of Hg and Se, with guillemots showing an increasing east-west gradient of Hg and Se, while kittiwakes showing a decreasing east-west gradient of Se. While sample sizes in the present study remain limited and should now be increased in a wider and multi-species perspective, obtained results highlight clear patterns and raise new questions about Se dynamics in marine food webs, suggesting that different seabird populations and species may be exposed to different levels of Hg toxicity risk depending on their spatial distribution. Moreover, guillemots appear to be at higher risk than kittiwakes in both oceans, due to lower Se protection. Our study thus highlights the importance of considering Hg and Se levels when comparing Hg toxicity between species or populations.

Spatial distribution of Hg and Se in the Arctic and subarctic

As predicted, Hg increased east-west from the European Arctic to the Canadian Arctic, but only in guillemots. This higher Hg concentration in guillemots at lower longitudes is in accordance with the gradient previously reported and observed in all auk species (Albert et al. 2019; Albert et al. 2021), most likely as a result of different Hg spatial availability in the environment. However, we did not find such a spatial variation in Hg concentrations for kittiwakes. This difference between the two studied species could be related to differences in their trophic ecology. Indeed, kittiwakes are known to feed (i) at the ocean surface during day and night, on pelagic and on mesopelagic prey respectively, thanks to diel vertical migration of mesopelagic prey (Hatch et al. 2020). Such variability in their foraging ecology could blur the Hg spatial trends across kittiwake Arctic distribution. Even if guillemots are known to target prey from midwaters to the bottom, from depths of 7 m to a maximum of 200 m (Patterson et al. 2022), and on mesopelagic prey at night, they appear to be a better indicator of the Hg spatial variations in the Arctic than kittiwakes.

About Se, this is the first time that the spatial variation of Se in wildlife has been studied across the Arctic. The opposite gradient found for both species, with higher Se concentrations for guillemots and

lower Se concentrations for kittiwakes at lower longitudes, suggest that the Se gradients we have found do not depend on Se spatial variability in the environment. They most likely depend (i) on the diet of the species, since Se enters the organism through food, as does Hg, and (ii) on the physical-chemical form of Se in the different prey, which influences its bioavailability to predators (e.g., Lemly and Smith 1987; Dumont et al. 2006). This result highlights the importance of examining Se gradients independently for each species. In the Southern Ocean, a clear gradient of Se concentration was reported in skuas, with lower Se concentrations at lower latitudes (Carravieri et al. 2017), likely as a result of the latitudinal stratification of water masses around the Antarctic continent. In the Arctic, the heterogeneity of the oceanographic circulation, together with the results found in this work, calls for a better evaluation of Se spatial distribution.

These spatial results in Hg and Se concentrations suggest (i) a lower Hg toxicity risk in the European Arctic for guillemots due to the lower Hg concentration observed, and (ii) most likely a higher protection by Se for kittiwakes in the European Arctic due to the higher Se concentration observed. Our results nonetheless highlight the importance of examining Hg and Se at the same time when evaluating Hg toxicity risks, since it is known that Hg can affect reproduction and population dynamics, especially when Se concentrations are low (Goutte et al. 2014a; Goutte et al. 2014b). For instance, guillemots from colonies at lower longitudes show Hg concentrations above the Hg toxicity risk threshold (corresponding to moderate risks, Ackerman et al. 2016, Figure 1 and Table 1), and lower Se:Hg than at higher latitudes, and this could give an explanation for the contrasting breeding success found in guillemot colonies across the Arctic (Frederiksen et al. 2021), since higher breeding success was reported for those colonies where we found higher Se:Hg. To our knowledge, there are no multi-population studies evaluating breeding success along with kittiwake Arctic distribution, but we cannot ignore that those populations with higher Se concentrations could also experience a toxic effect of Se, as it could happen for every trace element when there is an excess, especially during embryonic development which could then affect the species breeding success (Outridge et al. 1999; Spallholz and Hoffman 2002). Hence, investigating the link between Se:Hg and population trends will be crucial in order to further examine adverse impacts of Hg and the importance of Se as a protector against Hg

toxicity or as a toxic element. Moreover, this demonstrates that international monitoring programs that are focused on Hg should now include Se for reliable projection of Hg and Se toxicity risk and subsequent Hg mitigation measures.

Inter-specific, colony and ocean basin differences in Hg and Se concentrations, and in Se:Hg molar ratios

The absence of significant differences in Hg concentrations between guillemots and kittiwakes in the Atlantic-Arctic and in the Pacific-Arctic do not follow our expectations based on the results reported by Chastel et al. 2022, where guillemots showed lower Hg concentrations than kittiwakes. In the present study, the absence of differences in Hg concentrations between both species for most of the colonies, and the different trends found between Greenland and the Svalvbard archipelago colonies (with lower Hg concentrations for guillemots than kittiwakes only in Isfjorden, Alkefjellet and Bjørnøya, from the Svalbard archipelago; and higher Hg concentrations in the two colonies of west Greenland, i.e., Thule and Kippaku), may be due to the variability in the foraging ecology of both species among colonies. Brünnich's guillemots are considered one of the deepest divers of all birds in the northern hemisphere (Gaston & Hipfner, 2020), and the highest Hg concentrations have been found in their benthic prey (Braune et al. 2014) as a consequence of a greater input of MeHg to food webs below the mixed layer with a peak of MeHg in the aphotic zone (>100 m; Heimbürger et al. 2010; Blum et al. 2013). However, a recent study showed some variability in diving depth among guillemot colonies (e.g., Bonnet-Lebrun et al. 2021), which could partly imply differences in Hg concentrations among colonies. On their own, kittiwakes are surface predators, but they can also feed on prey from the deep ocean when they approach the surface at night (Hatch et al. 2020), and they can also feed along glacier fronts (Bertrand et al. 2021) where Hg concentrations could be higher (Hawkings et al. 2021). The differences we found among colonies may suggest differences in Hg toxic effects between both species depending on the colony, such as affection in the immune system, induction of oxidative stress, alteration in reproduction, or in the modulation of the reproductive effort (Hoffman et al. 2011; Tartu et al. 2013; Fort et al. 2014; Amélineau et al. 2019; Teitelbaum et al. 2022), and hence differences in the species population dynamics. In addition, guillemots could see their foraging efficiency altered via Hg impact on the thyroid

axis, as found in Brünnich guillemots of the northern Hudson Bay (Esparza et al. 2022), since T3 concentrations can be associated with Hg concentrations, and high T3 may increase oxygen consumption during dives reducing their foraging time underwater (Elliott et al. 2015). This could be happening in Thule (Greenland) where guillemots show the highest Hg concentrations (Esparza et al. 2022). Furthermore, in studies performed in other kittiwake colonies in the Arctic, the variation in Hg concentrations seems to decrease as the breeding cycle progresses and to be sex-dependent, with males showing higher concentrations than females (Øverjordet et al. 2015b; Tartu et al. 2022). Thus, additional studies differentiating adults by breeding phase and sex when evaluating the pair Se-Hg would be necessary.

In contrast to Hg, Se concentrations within oceans, and in almost all colonies where both guillemots and kittiwakes were sampled, the results followed our expectations with significantly lower Se concentrations in guillemots than in kittiwakes within oceans (i.e., up to four times lower in the Atlantic-Arctic; Figure 2). These results follow what was found in other studies that showed lower Se concentrations for species or individuals with a coastal-influenced diet (AMAP 2018; Carravieri et al. 2020; Damseaux et al. 2021). However, Se concentrations measured in the blood of guillemots and kittiwakes are very different from the Se blood values already reported for the only polar seabird in which blood Hg and Se have been investigated together: the polar skua, which breeds in Antarctica (Goutte et al. 2014b; Carravieri et al. 2017). Guillemots showed twice the Hg but half the Se concentrations than found in polar skuas. This result suggests that guillemot populations have a higher risk of Hg toxicity than that observed in Antarctic polar skuas, which already showed long-term impacts on reproduction (Goutte et al. 2014b). Nevertheless, kittiwakes had twice the Hg and Se concentrations of polar skuas, and therefore both species show similar Se:Hg, suggesting kittiwakes could be as protected as polar skuas against Hg toxicity. Both guillemots and kittiwakes in the Arctic showed Se:Hg ratios higher than 1 (but lower in guillemots than in kittiwakes). If we assume that both species have 1:1 stoichiometries, guillemot populations would be less protected against Hg toxicity than kittiwake populations, contrary to what we would think if we only considered the absence of differences in Hg concentrations between both species mentioned before. Although additional investigations on more

individuals and more species should be performed to validate this hypothesis, our results show how species from the same region could be differently impacted by Hg through differences in Se intakes. Consequently, variations in diet, prey type, or foraging habitats could influence bird capacity to acquire Se which is physiologically required for protection against Hg toxicity.

Finally, the absence of differences in the Se:Hg between the Atlantic-Arctic and the Pacific-Arctic for guillemots and kittiwakes, highlights that the protection against Hg toxicity is in some way similar between both ocean basins, which should be taken into consideration for their protection at the population level.

Influence of trophic ecology on trace elements concentrations

The absence of consistent patterns between Hg and Se concentrations with $\delta^{15}N$ and $\delta^{13}C$ suggests that the trophic ecology itself does not explain the observed spatial differences in Hg and Se concentrations. The moderate linear increase in Hg concentrations with $\delta^{15}N$ we found in guillemots follows our expectations, most likely due to Hg biomagnification in food webs (Bargagli et al. 1998; Seco et al. 2021). However, the effect of $\delta^{15}N$ on Hg concentrations in kittiwakes was quadratic rather than linear, which does not demonstrate evidence of Hg biomagnification in this species. However, the respective effect of $\delta^{13}C$ and $\delta^{15}N$ on Hg and Se concentrations in both species, together with the effect of $\delta^{13}C$ on Se concentrations in kittiwakes, nonetheless point to some influence of the diet and foraging habitat on both trace element concentrations. The study of trace element concentrations and isotopic values in the prey of both species could now help to better understand the influence of the trophic ecology on Hg and Se concentrations in these two seabird species.

The differences between species in trace elements and isotopic values depending on the colony suggest (i) a variability in the foraging strategies of both species (Moody et al. 2012; Hovinen et al. 2019), and (ii) the difficulty to detect the effect of diet through $\delta^{15}N$ and $\delta^{13}C$ on trace element concentrations due to differences in $\delta^{15}N$ and $\delta^{13}C$ isotopic baseline throughout the distribution of the studied colonies, as

it is supported by Figure S2. However, spatial changes in the isotopic baseline of $\delta^{15}N$ and $\delta^{13}C$ (isoscapes) were not considered in this study due to the magnitude of the studied area.

Furthermore, it is possible that Hg and Se concentrations found in these species depend on other factors apart from the trophic ecology, either intrinsic factors such as sex or age (Blévin et al. 2013; Mills et al. 2022), or extrinsic ones such as their wintering distributions and ecology (Carravieri et al. 2014; Albert et al. 2021; Carravieri et al. 2023), that we did not evaluate or control in this study, which hinder a clear detection of the effect of the foraging ecology in trace element concentrations.

Future perspectives

Long-term dietary changes in guillemots and kittiwakes due to climate change could affect their exposure to contaminants and thus their risks of toxicity. The warmer waters and the retraction of the ice zone in the Arctic make Arctic species retract northwards while Boreal and Atlantic species expand to the Arctic zone. This "borealization" and "Atlantification" of the Arctic alter the community composition of lower and middle trophic levels (Fossheim et al. 2015; Kortsch et al. 2015), leading to changes in the diet of predators like seabirds. These changes in diet have already been observed in guillemots from Northern Hudson Bay (Gaston et al. 2003) and in kittiwakes from Svalbard (Vihtakari et al. 2018), as well as in other seabird species from the Arctic (Descamps et al. 2022). The lower nutritive value of Atlantic prey (Descamps et al. 2022) may amplify the energetic constraint imposed by Hg detoxification. This, together with the possible change of distribution and phenology of migratory species due to climate change (e.g., in guillemots, Patterson et al. 2021), could modify the exposure to Hg and Se concentrations. Thus, new evaluations of the exposure and risk associated with Hg and Se concentrations should be carried out as climate change and the "Atlantification" advances.

CONCLUSIONS

Here we study for the first time the spatial distribution of Hg and Se in two seabird species in the Arctic and subarctic regions, the Burnish's guillemot and the black-legged kittiwake. Differences in Hg and Se spatial distribution highlight the need to evaluate Hg and Se concentrations together when assessing Hg

toxicity risks. This is especially important for international monitoring programs focusing on Hg toxicity risks in marine predators and its mitigation measures. Moreover, the absence of a consistent pattern between Hg and Se with $\delta^{15}N$ and $\delta^{13}C$ suggests high variability in the foraging strategy of both species as well as high variability in $\delta^{15}N$ and $\delta^{13}C$ baselines over the large scale of the study. Other extrinsic and intrinsic factors could also be affecting Hg and Se concentrations (e.g., climate, sex, or age), thus further studies integrating these factors on more species and individuals are now needed to improve the knowledge about Se spatial trend in Arctic seabirds.

AUTHOR CONTRIBUTION

MC-F contributed to the data curation, methodology design, formal data analysis, and wrote the original drafts of the publication; JL contributed to the methodology design, and samples analysis; MB-F, CC and GG contributed to samples analysis; SD, AP and PB contributed to the methodology design; JF contributed to the conceptualization, methodology design, project administration through the ARCTOX network, funding acquisition for metal and isotopic analyses, and samples analysis; SC-D, SD, KE, KEE, AE, MG, DG, SH, NH, YK, ASK, YK, ML, SL, JFL, EL, MLM, FRM, WM, AM, AP, SP, JFP, TKR, HR, HS, AT, J-BT, TLT and AW contributed to resources (samples). All authors contributed critically to the revision and edition of the original draft and gave final approval for publication.

ACKNOWLEDGEMENTS

We are grateful to all the people involved in fieldwork at the different study sites, including Michael Toolie and David Akeya on St. Lawrence Island. We also thank the platforms “Analyses Elémentaires” and “Analyses Isotopiques” of LIENSs laboratory for isotope and trace element analyses, the “Cellule Géomatique” and Cécilia Pignon-Mussaud for mapping the data, and Julie Charrier for the drawings used in this publication. This study was funded by ANR MAMBA (ANR-16-TERC-0004) and is part of the ARCTOX international initiative (https://arctox.cnrs.fr). This is also a contribution to the ILETOP (ANR-16-CE34-0005) and ARCTIC-STRESSORS (ANR-20-CE34-0006) projects and to the French Polar Institute ADACLIM program (Pgr. 388). Thanks are due to the CPER (Contrat de Projet Etat-Région) and the FEDER (Fonds Européen de Développement Régional) for funding the AMAs, ICPs

and IRMSs of LIENSs laboratory. MCF was supported by the H2020 Marie Skłodowska Curie Actions (H2020-MSCA-IF-2020, ref. 101024166), PB is an honorary member of the IUF (Institut Universitaire de France). Sampling in Norwegian, Icelandic and Russian sites was supported by the SEATRACK project (www.seapop.no/en/seatrack/) funded by the Norwegian Ministry of Climate and Environment, the Norwegian Ministry of Foreign Affairs, Offshore Norge along with eight energy companies and the Norwegian Research Council (grant #192141). Sampling on Middleton Island was funded by the French Polar Institute 1162 program. St. Lawrence Island sampling was funded by the North Pacific Research Board (NPRB #1612-9) and the Japan Society for the Promotion of Science KAKENHI grant number JP16H02705, and the Arctic Challenge for Sustainability (ArCS) program of the Japan Ministry of Education, Culture, Sports, Science and Technology (MEXT). East Greenland sampling was funded by the French Polar Institute (IPEV - ADACLIM program 388). Samples from the Gannet Islands were collected with support from Environment and Climate Change Canada (core funding) and Acadia University (Grant 41-0-205561). Field work in St. Lawrence Island was conducted under the following permissions/permits: Native Village of Savoonga, Kukulget Land Crossing Permit, UAF IACUC protocol #470122, USFWS scientific collection permit #MB70337A, master banding permit #23350, and ADFG permit #16-089. Greenlandic samples were collected under the permit issue by the Government of Greenland (Dept. Fisheries, Hunting and Agriculture permit, ref. 5732726 and 1986082). Norwegian samples were collected under the permit issued by the Norwegian Food Authorities (FOTS ID 6291 and 8482). Samples from Middleton Island were collected under the approval of the USGS Alaska Science Centre Animal Care and Use Committee, in accordance with US law and under permits from the US Fish and Wildlife Service and the State of Alaska.

DATA ACCESSIBILITY

All data are already archived on the ARCTOX database and accessible upon request at http://arctox.cnrs.fr/en/work-area

BIBLIOGRAPHY

Ackerman JT, Eagles-Smith CA, Herzog MP, Hartman CA, Peterson SH, Evers DC, Jackson AK, Elliott JE, Vander Pol SS, Bryan CE (2016) Avian mercury exposure and toxicological risk across western North America: A synthesis. Sci Total Environ 568:749–769. https://doi.org/10.1016/j.scitotenv.2016.03.071

Albert C, Bråthen V, Descamps S, Anker-Nilssen T, Cherenkov A, Christensen-Dalsgaard S, Danielsen J, Erikstad K, Gavrilo M, Hanssen S, Helgason H, Jónsson J, Kolbeinsson Y, Krasnov Y, Langset M, Lorentzen E, Olsen B, Reiertsen T, Strøm H, Systad G, Tertitski G, Thompson P, Thórarinsson T, Bustamante P, Moe B, Fort J (2021) Inter-annual variation in winter distribution affects individual seabird contamination with mercury. Mar Ecol Prog Ser 676:243–254. https://doi.org/10.3354/meps13793

Albert C, Renedo M, Bustamante P, Fort J (2019) Using blood and feathers to investigate large-scale Hg contamination in Arctic seabirds: A review. Environ Res 177:108588. https://doi.org/10.1016/j.envres.2019.108588

AMAP (2011) AMAP Assessment 2011: Mercury in the Arctic. Arctic Monitoring and Assessment Programme (AMAP). Oslo

AMAP (2018) AMAP Assessment 2018: Biological Effects of Contaminants on Arctic Wildlife and Fish. Arctic Monitoring and Assessment Programme (AMAP), Tromsø, Norway (www.amap.no)

Amélineau F, Grémillet D, Harding AMA, Walkusz W, Choquet R, Fort J (2019) Arctic climate change and pollution impact little auk foraging and fitness across a decade. Sci Rep 9:1014. https://doi.org/10.1038/s41598-018-38042-z

Bargagli R, Monaci F, Sanchez-Hernandez J, Cateni D (1998) Biomagnification of mercury in an Antarctic marine coastal food web. Mar Ecol Prog Ser 169:65–76. https://doi.org/10.3354/meps169065

Bates D, Mächler M, Bolker B, Walker S (2015) Fitting Linear Mixed-Effects Models Using **lme4**. J Stat Softw 67. https://doi.org/10.18637/jss.v067.i01

Bertrand P, Strøm H, Bêty J, Steen H, Kohler J, Vihtakari M, van Pelt W, Yoccoz N, Hop H, Harris S, Patrick S, Assmy P, Wold A, Duarte P, Moholdt G, Descamps S (2021) Feeding at the front line:

interannual variation in the use of glacier fronts by foraging black-legged kittiwakes. Mar Ecol Prog Ser 677:197–208. https://doi.org/10.3354/meps13869

Blévin P, Carravieri A, Jaeger A, Chastel O, Bustamante P, Cherel Y (2013) Wide Range of Mercury Contamination in Chicks of Southern Ocean Seabirds. PLoS One 8:e54508. https://doi.org/10.1371/journal.pone.0054508

Blum JD, Popp BN, Drazen JC, Anela Choy C, Johnson MW (2013) Methylmercury production below the mixed layer in the North Pacific Ocean. Nat Geosci 6:879–884. https://doi.org/10.1038/ngeo1918

Bonnet-Lebrun A-S, Larsen T, Frederiksen M, Fox D, le Bouard F, Boutet A, Þórarinsson ÞL, Kolbeinsson Y, Deville T, Ratcliffe N (2021) Effects of competitive pressure and habitat heterogeneity on niche partitioning between Arctic and boreal congeners. Sci Rep 11:22133. https://doi.org/10.1038/s41598-021-01506-w

Braune BM, Gaston AJ, Elliott KH, Provencher JF, Woo KJ, Chambellant M, Ferguson SH, Letcher RJ (2014) Organohalogen contaminants and total mercury in forage fish preyed upon by thick-billed murres in northern Hudson Bay. Mar Pollut Bull 78:258–266. https://doi.org/10.1016/j.marpolbul.2013.11.003

Buchheister A, Latour RJ (2010) Turnover and fractionation of carbon and nitrogen stable isotopes in tissues of a migratory coastal predator, summer flounder (*Paralichthys dentatus*). Canadian Journal of Fisheries and Aquatic Sciences 67:445–461. https://doi.org/10.1139/F09-196

Burnham KP, Anderson DR (2002) Model selection and multimodel inference: a practical information-theoretic approach, 2nd edn. Springer, New York

Carravieri A, Burthe SJ, de la Vega C, Yonehara Y, Daunt F, Newell MA, Jeffreys RM, Lawlor AJ, Hunt A, Shore RF, Pereira MG, Green JA (2020) Interactions between Environmental Contaminants and Gastrointestinal Parasites: Novel Insights from an Integrative Approach in a Marine Predator. Environ Sci Technol 54:8938–8948. https://doi.org/10.1021/acs.est.0c03021

Carravieri A, Cherel Y, Blévin P, Brault-Favrou M, Chastel O, Bustamante P (2014) Mercury exposure in a large subantarctic avian community. Environmental Pollution 190:51–57. https://doi.org/10.1016/j.envpol.2014.03.017

Carravieri A, Cherel Y, Brault-Favrou M, Churlaud C, Peluhet L, Labadie P, Budzinski H, Chastel O, Bustamante P (2017) From Antarctica to the subtropics: Contrasted geographical concentrations of selenium, mercury, and persistent organic pollutants in skua chicks (*Catharacta spp.*). Environmental Pollution 228:464–473. https://doi.org/10.1016/j.envpol.2017.05.053

Carravieri A, Lorioux S, Angelier F, Chastel O, Albert C, Bråthen VS, Brisson-Curadeau É, Clairbaux M, Delord K, Giraudeau M, Perret S, Poupart T, Ribout C, Viricel-Pante A, Grémillet D, Bustamante P, Fort J (2023) Carryover effects of winter mercury contamination on summer concentrations and reproductive performance in little auks. Environmental Pollution 318:120774. https://doi.org/10.1016/j.envpol.2022.120774

Carvalho PC, Bugoni L, McGill RAR, Bianchini A (2013) Metal and selenium concentrations in blood and feathers of petrels of the genus Procellaria. Environ Toxicol Chem n/a-n/a. https://doi.org/10.1002/etc.2204

Chastel O, Fort J, Ackerman JT, Albert C, Angelier F, Basu N, Blévin P, Brault-Favrou M, Bustnes JO, Bustamante P, Danielsen J, Descamps S, Dietz R, Erikstad KE, Eulaers I, Ezhov A, Fleishman AB, Gabrielsen GW, Gavrilo M, Gilchrist G, Gilg O, Gíslason S, Golubova E, Goutte A, Grémillet D, Hallgrimsson GT, Hansen ES, Hanssen SA, Hatch S, Huffeldt NP, Jakubas D, Jónsson JE, Kitaysky AS, Kolbeinsson Y, Krasnov Y, Letcher RJ, Linnebjerg JF, Mallory M, Merkel FR, Moe B, Montevecchi WJ, Mosbech A, Olsen B, Orben RA, Provencher JF, Ragnarsdottir SB, Reiertsen TK, Rojek N, Romano M, Søndergaard J, Strøm H, Takahashi A, Tartu S, Thórarinsson TL, Thiebot J-B, Will AP, Wilson S, Wojczulanis-Jakubas K, Yannic G (2022) Mercury contamination and potential health risks to Arctic seabirds and shorebirds. Science of The Total Environment 844:156944. https://doi.org/10.1016/j.scitotenv.2022.156944

Cipro CVZ, Cherel Y, Caurant F, Miramand P, Méndez-Fernandez P, Bustamante P (2014) Trace elements in tissues of white-chinned petrels (*Procellaria aequinoctialis*) from Kerguelen waters, Southern Indian Ocean. Polar Biol 37:763–771. https://doi.org/10.1007/s00300-014-1476-z

Cutter GA, Bruland KW (1984) The marine biogeochemistry of selenium: A re-evaluation. Limnol Oceanogr 29:1179–1192. https://doi.org/10.4319/lo.1984.29.6.1179

Cuvin-Aralar MaLA, Furness RW (1991) Mercury and selenium interaction: A review. Ecotoxicol Environ Saf 21:348–364. https://doi.org/10.1016/0147-6513(91)90074-Y

Damseaux F, Siebert U, Pomeroy P, Lepoint G, Das K (2021) Habitat and resource segregation of two sympatric seals in the North Sea. Science of The Total Environment 764:142842. https://doi.org/10.1016/j.scitotenv.2020.142842

Descamps S, Wojczulanis-Jakubas K, Jakubas D, Vihtakari M, Steen H, Karnovsky NJ, Welcker J, Hovinen J, Bertrand P, Strzelewicz A, Skogseth R, Kidawa D, Boehnke R, Błachowiak-Samołyk K (2022) Consequences of Atlantification on a Zooplanktivorous Arctic Seabird. Front Mar Sci 9. https://doi.org/10.3389/fmars.2022.878746

Dumont E, Vanhaecke F, Cornelis R (2006) Selenium speciation from food source to metabolites: a critical review. Anal Bioanal Chem 385:1304–1323. https://doi.org/10.1007/s00216-006-0529-8

Elliott KH, Hare JF, Le Vaillant M, Gaston AJ, Ropert-Coudert Y, Anderson WG (2015) Ageing gracefully: physiology but not behaviour declines with age in a diving seabird. Funct Ecol 29:219–228. https://doi.org/10.1111/1365-2435.12316

Esparza I, Elliott KH, Choy ES, Braune BM, Letcher RJ, Patterson A, Fernie KJ (2022) Mercury, legacy and emerging POPs, and endocrine-behavioural linkages: Implications of Arctic change in a diving seabird. Environ Res 212:113190. https://doi.org/10.1016/j.envres.2022.113190

Espinasse B, Hunt BP V., Batten SD, Pakhomov EA (2020) Defining isoscapes in the Northeast Pacific as an index of ocean productivity. Global Ecology and Biogeography 29:246–261. https://doi.org/10.1111/geb.13022

Fort J, Robertson GJ, Grémillet D, Traisnel G, Bustamante P (2014) Spatial Ecotoxicology: Migratory Arctic Seabirds Are Exposed to Mercury Contamination While Overwintering in the Northwest Atlantic. Environ Sci Technol 48:11560–11567. https://doi.org/10.1021/es504045g

Fossheim M, Primicerio R, Johannesen E, Ingvaldsen RB, Aschan MM, Dolgov A V. (2015) Recent warming leads to a rapid borealization of fish communities in the Arctic. Nat Clim Chang 5:673–677. https://doi.org/10.1038/nclimate2647

Frederiksen M, Descamps S, Elliott K, Gaston A, Huffeldt N, Kolbeinsson Y, Linnebjerg J, Lorentzen E, Merkel F, Strøm H, Thórarinsson T (2021) Spatial variation in vital rates and population growth

of thick-billed murres in the Atlantic Arctic. Mar Ecol Prog Ser 672:1–13. https://doi.org/10.3354/meps13823

Gaston AJ, Hipfner JM (2020) Thick-billed Murre (Uria lomvia). In: Billerman SM (ed) Birds of the World. Cornell Lab of Ornithology

Gaston AJ, Woo K, Hipfner JM (2003) Trends in Forage Fish Populations in Northern Hudson Bay since 1981, as Determined from the Diet of Nestling Thick-billed Murres, *Uria lomvia*; Arctic 56. https://doi.org/10.14430/arctic618

González-Solís J, Sanpera C, Ruiz X (2002) Metals and selenium as bioindicators of geographic and trophic segregation in giant petrels *Macronectes spp.* Mar Ecol Prog Ser 244:257–264. https://doi.org/10.3354/meps244257

Goutte A, Barbraud C, Meillère A, Carravieri A, Bustamante P, Labadie P, Budzinski H, Delord K, Cherel Y, Weimerskirch H, Chastel O (2014a) Demographic consequences of heavy metals and persistent organic pollutants in a vulnerable long-lived bird, the wandering albatross. Proceedings of the Royal Society B: Biological Sciences 281:20133313. https://doi.org/10.1098/rspb.2013.3313

Goutte A, Bustamante P, Barbraud C, Delord K, Weimerskirch H, Chastel O (2014b) Demographic responses to mercury exposure in two closely related Antarctic top predators. Ecology 95:1075–1086. https://doi.org/10.1890/13-1229.1

Hatch SA, Robertson GJ, Baird PH (2020) Black-legged Kittiwake (*Rissa tridactyla*). In: Billerman SM (ed) Birds of the World. Cornell Lab of Ornithology

Hawkings JR, Linhoff BS, Wadham JL, Stibal M, Lamborg CH, Carling GT, Lamarche-Gagnon G, Kohler TJ, Ward R, Hendry KR, Falteisek L, Kellerman AM, Cameron KA, Hatton JE, Tingey S, Holt AD, Vinšová P, Hofer S, Bulínová M, Větrovský T, Meire L, Spencer RGM (2021) Large subglacial source of mercury from the southwestern margin of the Greenland Ice Sheet. Nat Geosci 14:496–502. https://doi.org/10.1038/s41561-021-00753-w

Heimbürger L-E, Cossa D, Marty J-C, Migon C, Averty B, Dufour A, Ras J (2010) Methyl mercury distributions in relation to the presence of nano- and picophytoplankton in an oceanic water column

(Ligurian Sea, North-western Mediterranean). Geochim Cosmochim Acta 74:5549–5559. https://doi.org/10.1016/j.gca.2010.06.036

Hoffman DJ, Eagles-Smith CA, Ackerman JT, Adelsbach TL, Stebbins KR (2011) Oxidative stress response of Forster's terns (Sterna forsteri) and Caspian terns (*Hydroprogne caspia*) to mercury and selenium bioaccumulation in liver, kidney, and brain. Environ Toxicol Chem 30:920–929. https://doi.org/10.1002/etc.459

Hovinen J, Tarroux A, Ramírez F, Forero M, Descamps S (2019) Relationships between isotopic ratios, body condition and breeding success in a High Arctic seabird community. Mar Ecol Prog Ser 613:183–195. https://doi.org/10.3354/meps12886

Jackson AL, Inger R, Parnell AC, Bearhop S (2011) Comparing isotopic niche widths among and within communities: SIBER – Stable Isotope Bayesian Ellipses in R. Journal of Animal Ecology 80:595–602. https://doi.org/10.1111/j.1365-2656.2011.01806.x

Kortsch S, Primicerio R, Fossheim M, Dolgov A V., Aschan M (2015) Climate change alters the structure of arctic marine food webs due to poleward shifts of boreal generalists. Proceedings of the Royal Society B: Biological Sciences 282:20151546. https://doi.org/10.1098/rspb.2015.1546

Lemly AD, Smith GJ (1987) Aquatic cycling of selenium: implications for fish and wildlife.

Manceau A, Gaillot A-C, Glatzel P, Cherel Y, Bustamante P (2021) In Vivo Formation of HgSe Nanoparticles and Hg–Tetraselenolate Complex from Methylmercury in Seabirds—Implications for the Hg–Se Antagonism. Environ Sci Technol 55:1515–1526. https://doi.org/10.1021/acs.est.0c06269

McMahon KW, Hamady LL, Thorrold SR (2013) A review of ecogeochemistry approaches to estimating movements of marine animals. Limnol Oceanogr 58:697–714

Mehdi Y, Hornick J-L, Istasse L, Dufrasne I (2013) Selenium in the Environment, Metabolism and Involvement in Body Functions. Molecules 18:3292–3311. https://doi.org/10.3390/molecules18033292

Mills WF, Ibañez AE, Bustamante P, Carneiro APB, Bearhop S, Cherel Y, Mariano-Jelicich R, McGill RAR, Montalti D, Votier SC, Phillips RA (2022) Spatial and sex differences in mercury

contamination of skuas in the Southern Ocean. Environmental Pollution 297:118841. https://doi.org/10.1016/J.ENVPOL.2022.118841

Monteiro LR, Furness RW (2001) Kinetics, Dose−Response, and Excretion of Methylmercury in Free-Living Adult Cory's Shearwaters. Environ Sci Technol 35:739–746. https://doi.org/10.1021/es000114a

Moody AT, Hobson KA, Gaston AJ (2012) High-arctic seabird trophic variation revealed through long-term isotopic monitoring. J Ornithol 153:1067–1078. https://doi.org/10.1007/s10336-012-0836-0

Newsome SD, Martínez del Rio C, Bearhop S, Phillips DL (2007) A niche for isotopic ecology. Front Ecol Environ 5:429–436

Nigro M, Leonzio C (1996) Intracellular storage of mercury and selenium in different marine vertebrates. Mar Ecol Prog Ser 135:137–143. https://doi.org/10.3354/meps135137

Outridge PM, Scheuhammer AM, Fox GA, Braune BM, White LM, Gregorich LJ, Keddy C (1999) An assessment of the potential hazards of environmental selenium for Canadian water birds. Environmental Reviews 7:81–96. https://doi.org/10.1139/a99-009

Øverjordet IB, Gabrielsen GW, Berg T, Ruus A, Evenset A, Borgå K, Christensen G, Lierhagen S, Jenssen BM (2015a) Effect of diet, location and sampling year on bioaccumulation of mercury, selenium and cadmium in pelagic feeding seabirds in Svalbard. Chemosphere 122:14–22. https://doi.org/10.1016/j.chemosphere.2014.10.060

Øverjordet IB, Kongsrud MB, Gabrielsen GW, Berg T, Ruus A, Evenset A, Borgå K, Christensen G, Jenssen BM (2015b) Toxic and essential elements changed in black-legged kittiwakes (*Rissa tridactyla*) during their stay in an Arctic breeding area. Science of The Total Environment 502:548–556. https://doi.org/10.1016/j.scitotenv.2014.09.058

Patterson A, Gilchrist H, Gaston A, Elliott K (2021) Northwest range shifts and shorter wintering period of an Arctic seabird in response to four decades of changing ocean climate. Mar Ecol Prog Ser 679:163–179. https://doi.org/10.3354/meps13890

Patterson A, Gilchrist HG, Robertson GJ, Hedd A, Fifield DA, Elliott KH (2022) Behavioural flexibility in an Arctic seabird using two distinct marine habitats to survive the energetic constraints of winter. Mov Ecol 10:45. https://doi.org/10.1186/s40462-022-00344-3

R Core Team (2021) R: A language and environment for statistical computing. R Foundation for Statistical Computing, Vienna, Austria. URL https://www.R-project.org/

Ralston NVC, Raymond LJ (2018) Mercury's neurotoxicity is characterized by its disruption of selenium biochemistry. Biochimica et Biophysica Acta (BBA) - General Subjects 1862:2405–2416. https://doi.org/10.1016/j.bbagen.2018.05.009

Renedo M, Amouroux D, Albert C, Bérail S, Bråthen VS, Gavrilo M, Grémillet D, Helgason HH, Jakubas D, Mosbech A, Strøm H, Tessier E, Wojczulanis-Jakubas K, Bustamante P, Fort J (2020) Contrasting Spatial and Seasonal Trends of Methylmercury Exposure Pathways of Arctic Seabirds: Combination of Large-Scale Tracking and Stable Isotopic Approaches. Environ Sci Technol 54:13619–13629. https://doi.org/10.1021/acs.est.0c03285

Seco J, Aparício S, Brierley AS, Bustamante P, Ceia FR, Coelho JP, Philips RA, Saunders RA, Fielding S, Gregory S, Matias R, Pardal MA, Pereira E, Stowasser G, Tarling GA, Xavier JC (2021) Mercury biomagnification in a Southern Ocean food web. Environmental Pollution 275:116620. https://doi.org/10.1016/j.envpol.2021.116620

Sen IS, Peucker-Ehrenbrink B (2012) Anthropogenic disturbance of element cycles at the Earth's surface. Environ Sci Technol 46:8601–8609. https://doi.org/10.1021/es301261x

Smith RA, Yurkowski DJ, Parkinson KJL, Fort J, Hennin HL, Gilchrist HG, Hobson KA, Mallory ML, Danielsen J, Garbus SE, Hanssen SA, Jónsson JE, Latty CJ, Magnúsdóttir E, Moe B, Parsons GJ, Sonne C, Tertitski G, Love OP (2021) Environmental and life-history factors influence inter-colony multidimensional niche metrics of a breeding Arctic marine bird. Sci Total Environ 796:148935. https://doi.org/10.1016/j.scitotenv.2021.148935

Spallholz JE, Hoffman DJ (2002) Selenium toxicity: cause and effects in aquatic birds. Aquatic Toxicology 57:27–37. https://doi.org/10.1016/S0166-445X(01)00268-5

Tan SW, Meiller JC, Mahaffey KR (2009) The endocrine effects of mercury in humans and wildlife. Crit Rev Toxicol 39:228–269. https://doi.org/10.1080/10408440802233259

Tartu S, Blévin P, Bustamante P, Angelier F, Bech C, Bustnes JO, Chierici M, Fransson A, Gabrielsen GW, Goutte A, Moe B, Sauser C, Sire J, Barbraud C, Chastel O (2022) A U-Turn for Mercury

Concentrations over 20 Years: How Do Environmental Conditions Affect Exposure in Arctic Seabirds? Environ Sci Technol 56:2443–2454. https://doi.org/10.1021/acs.est.1c07633

Tartu S, Goutte A, Bustamante P, Angelier F, Moe B, Clément-Chastel C, Bech C, Gabrielsen GW, Bustnes JO, Chastel O (2013) To breed or not to breed: endocrine response to mercury contamination by an Arctic seabird. Biol Lett 9:20130317. https://doi.org/10.1098/rsbl.2013.0317

Teitelbaum CS, Ackerman JT, Hill MA, Satter JM, Casazza ML, De La Cruz SEW, Boyce WM, Buck EJ, Eadie JM, Herzog MP, Matchett EL, Overton CT, Peterson SH, Plancarte M, Ramey AM, Sullivan JD, Prosser DJ (2022) Avian influenza antibody prevalence increases with mercury contamination in wild waterfowl. Proceedings of the Royal Society B: Biological Sciences 289. https://doi.org/10.1098/rspb.2022.1312

Vihtakari M, Welcker J, Moe B, Chastel O, Tartu S, Hop H, Bech C, Descamps S, Gabrielsen GW (2018) Black-legged kittiwakes as messengers of Atlantification in the Arctic. Sci Rep 8:1178. https://doi.org/10.1038/s41598-017-19118-8

Wolfe MF, Schwarzbach S, Sulaiman RA (1998) Effects of mercury on wildlife: A comprehensive review. Environ Toxicol Chem 17:146–160. https://doi.org/10.1002/etc.5620170203

Zuur AF, Leno EN, Walker NJ, Saveliev AA, Smith GM (2009) Limitations of Linear Regression Applied on Ecological Data. In: Mixed effects models and extensions in ecology with R. Springer New York, New York, NY, pp 11–33

Table 1. Mean ± SD whole blood Hg and Se concentrations (µg g^{-1} dw), Se:Hg molar ratios, and $\delta^{15}N$ and $\delta^{13}C$ values (‰) in 13 populations of Brünnich's guillemots (BG; *Uria lomvia)* and 13 populations of black-legged kittiwakes (BLK; *Rissa tridactyla)* from the Arctic and subarctic regions ordered by ascending longitude degrees. Ocean basin of belonging, longitude, latitude, and years of sampling are specified. Significant differences between species obtained from Mann-Whitney tests are shown with asterisks (*<0.5, **<0.01, ***<0.001).

					Hg		**Se**		**Se:Hg**		**$\delta^{15}N$**		**$\delta^{13}C$**	
		Long	**Lat**	**Years of sampling**	**BG**	**BLK**	**BG**	**BLK**	**BG**	**BLK**	**BG**	**BLK**	**BG**	**BLK**
Pacific-Arctic	**Saint Lawrence Is. (SL; USA)**	-170.2	63.4	2016	1.13±0.52 n=5	0.87±0.43 n=4	22.71±13.12 n=5 *	74.23±24.37 n=3	51.7±24.3 n=5 *	183.4±74.4 n=3	17.3±0.4 n=5	15.9±1.4 n=4	-18.0±0.2 n=5 *	-18.5±0.2 n=4
	Middleton Is. (MID; USA)	-146.3	59.4	2016	-	1.28±0.21 n=5	-	76.59±9.13 n=5	-	155.3±30.8 n=5	-	14.9±0.2 n=5	-	-20.8±0.3 n=5
Atlantic-Arctic	**Coats Island (CI; Canada)**	-83.1	62.5	2016	1.20±0.20 n=5	-	19.23±5.95 n=5	-	40.6±9.5 n=5	-	14.8±0.3 n=5	-	-20.3±0.1 n=5	-
	Thule (THU; Greenland)	-69.2	77.5	2015	2.43±1.04 n=5 *	0.94±0.15 n=4	32.94±8.53 n=5	42.55±6.33 n=5	39.2±18.6 n=5 *	108.8±10.2 n=4	13.7±0.4 n=5 *	12.9±0.3 n=4	-20.2±0.1 n=5	-20.8±0.4 n=4
	Kippaku (KIP; Greenland)	-56.6	73.7	BG: 2016 BLK: 2015	1.34±0.52 n=5 *	0.62±0.09 n=5	29.55±5.64 n=5 **	76.82±8.20 n=5	63.3±23.7 n=5 **	323.5±68.8 n=5	13.8±0.2 n=5	14.9±0.1 n=5	-20.0±0.1 n=5	-20.2±0.1 n=5
	Gannets Island (GI; Canada)	-56.6	53.9	2015	2.04±0.74 n=5	-	43.94±9.50 n=5	-	61.9±26.1 n=5	-	13.9±0.3 n=5	-	-19.7±0.2 n=5	-
	Gull Island (GUL; Canada)	-53.0	48.0	2017	-	1.09±0.35 n=5	-	104.30±35.45 n=5	-	253.9±71.6 n=5	-	12.2±0.6 n=5	-	-21.1±0.3 n=5
	Dunholm (DU; Greenland)	-22.6	69.9	2017	-	1.00±0.32 n=5	-	93.91±6.65 n=5	-	261.5±92.8 n=5	-	14.2±0.2 n=5	-	-22.1±0.1 n=5
	Langanes (LAN; Iceland)	-16.0	66.2	2016	0.72±0.11 n=5	1.1±0.53 n=5	20.75±3.28 n=5 **	97.92±30.42 n=5	73.3±7.4 n=5 **	271.3±171.2 n=5	11.8±0.1 n=5	12.1±0.5 n=5	-20.5±0.2 n=5	-20.7±0.2 n=5
	Jan Mayen (JM; Norway)	-8.3	71.0	2016	1.52±0.31 n=5	-	10.75±2.70 n=5	-	18.9±7.2 n=5	-	12.2±0.2 n=5	-	-22.0±0.1 n=5	-

Anda (AND; Norway)	15.2	69.0	2017	-	0.95±0.35 n=5	-	141.62±33.06 n=5	-	392.7±66.7 n=5	-	12.3±0.3 n=5	-	-20.5±0.1 n=5
Isfjorden (ISF; Norway)	15.5	78.3	2016	0.74±0.38 n=5 **	1.70±0.62 n=5	20.09±4.50 n=5 **	148.72±19.08 n=5	89.9±56.5 n=5 *	244.4±77.5 n=5	13.0±0.6 n=5	12.2±0.6 n=5	-21.0±0.1 n=5	-20.9±0.2 n=5
Alkefjellet (ALK; Norway)	18.5	79.6	2016	0.42±0.24 n=5 *	0.93±0.25 n=5	27.89±6.25 n=5 **	99.68±19.24 n=5	200.8±74.5 n=5	303.6±160.6 n=5	13.1±0.8 n=5	13.3±0.4 n=5	-20.8±0.3 n=5	-21.1±0.1 n=5
Bjørnøya (BJO; Norway)	19.0	74.5	2016	0.22±0.07 n=5 **	0.56±0.06 n=5	14.80±3.14 n=5 *	42.19±11.87 n=3	185.0±65.2 n=5	190.6±60.1 n=3	12.4±0.5 n=5	13.0±0.4 n=5	-21.1±0.1 n=5	-21.1±0.1 n=5
Hornøya (HOR; Norway)	31.2	70.4	2016	0.94±0.12 n=5	1.13±0.30 n=5	10.21±2.75 n=5 **	85.24±36.55 n=5	28.0±8.4 n=5 **	186.1±46.0 n=5	14.3±0.3 n=5	14.2±0.3 n=5	-20.5±0.1 n=5	-20.5±0.2 n=5
Gorodetski Cape (GC; Russia)	32.9	69.6	2015	0.77±0.04 n=5	-	20.50±5.47 n=5	-	67.9±18.4 n=5	-	14.3±0.2 n=5	-	-20.5±0.0 n=5	-
Cape Flora (CF; Russia)	50.1	80.0	2016	0.71±0.11 n=5	0.88±0.16 n=5	23.10±3.96 n=5 **	131.61±9.82 n=5	83.6±14.5 n=5 **	390.2±86.6 n=5	13.8±0.4 n=5	14.4±0.5 n=5	-21.8±0.5 n=5 **	-21.2±0.2 n=5

Table 2. Modelling the spatial variation of whole blood Hg and Se concentrations (µg.g^{-1} dw) and of Se:Hg molar ratios for Brünnich's guillemots (BG; *Uria lomvia*) and black-legged kittiwakes (BLK; *Rissa tridactyla*) from different colonies of the Atlantic-Arctic ocean. Colony and year were included as random factors. For each model we provide the number of parameters (K), the Akaike Information Criterion corrected for small sample size (AICc) value, and the ΔAICc value as the difference in AICc compared to the model with the lowest AICc value from its set of models (per trace element and species). From each set of models, we provide AICc values in ascending order. To reflect the effects of those factors from the best models (AICc lower than the null model and ΔAICc lower than two) we provide the regression functions and the confidence interval of their effects, as well as the variance ± SD of the random effects and the residuals. Only the first five models per set of models are shown (complete list of models in Table S1 in Supplementary Material).

								Random effects (Variance ± SD)		
		Model	**K**	**AICc**	**ΔAICc**	**Weight**	**Regression functions from the best model**	**Effect Confidence Interval (2.5 - 97.5%)**	**Colony**	**Year**	**Residual**
Blood Hg	BG	~ Long + $\delta^{15}N$	6	100.2	0	0.2	Hg ~ -1.230 - 0.009 x Long + 0.173 x $\delta^{15}N$	Long = -0.017 – -0.003; $\delta^{15}N$ = -0.040 – 0.425	0.2 ± 0.4	0.1 ± 0.3	0.2 ± 0.4
		~ Long	5	100.2	0.0	0.2	Hg ~ -1.125 - 0.009 x Long	Long = -0.016 – -0.004	0.1 ± 0.3	0.2 ± 0.4	0.2 ± 0.4
		~ Long : $\delta^{15}N$	5	100.3	0.2	0.1					
		~ Long + $\delta^{13}C$ + $(\delta^{13}C)^2$	7	100.8	0.6	0.1	Hg ~ 115.616 - 0.008 x Long + 10.988 x $\delta^{13}C$ + 0.263 x $(\delta^{13}C)^2$	Long = -0.014 – -0.002; $\delta^{13}C$ = 0.000 – 23.946; $(\delta^{13}C)^2$ = 0.004 – 0.567	0.1 ± 0.3	0.2 ± 0.4	0.2 ± 0.4
		~ Long + $\delta^{15}N$ + $\delta^{13}C$ + $(\delta^{13}C)^2$	8	100.9	0.7	0.1					
	BLK	~ $\delta^{15}N$ + $(\delta^{15}N)^2$	6	57.6	0	0.2	Hg ~ -20.975 + 3.226 x $\delta^{15}N$ - 0.118 x $(\delta^{15}N)^2$	$\delta^{15}N$ = 0.512 – 5.897; $(\delta^{15}N)^2$ = -0.220 – -0.016	0.1 ± 0.4	0.0 ± 0.0	0.1 ± 0.3
		~ d13C	5	58.3	0.7	0.2	Hg ~ 8.251 + 0.347 x $\delta^{13}C$	$\delta^{13}C$ = -0.054 – 0.750	0.1 ± 0.4	0.0 ± 0.0	0.1 ± 0.3
		~ 1	4	58.5	0.9	0.1					
		~ $\delta^{15}N$ + $\delta^{13}C$	6	59.1	1.5	0.1					
		~ $\delta^{13}C$ + $(\delta^{13}C)^2$	6	59.9	2.3	0.1					
Bl	BG	~ Long	5	414.8	0	0.2	Se ~ 23.995 - 0.084 x Long	Long = -0.212 – 0.015	52.0 ± 7.2	43.8 ± 6.6	30.9 ± 5.6

						Se ~ 24.160 - 0.005 x Long : $\delta^{15}N$	Long: $\delta^{15}N$ = -0.014 – 0.001	52.0 ± 7.2	47.2 ± 6.9	31.1 ± 5.6
	~ Long : $\delta^{15}N$	5	415.3	0.5	0.2					
	~ 1	4	415.4	0.5	0.2					
	~ δ13C	5	416.5	1.6	0.1					
	~ Long * $\delta^{15}N$	7	416.9	2.0	0.1					
	~ Long	5	509.1	0	0.1	Se ~ 99.567 + 0.421 x Long	Long = -0.083 – 0.923	943.2 ± 30.7	0.0 ± 0.0	552.0 ± 23.5
	~ Long + $\delta^{13}C$	6	509.3	0.1	0.1	Se ~ 617.064 + 0.455 x Long + 24.730 x $\delta^{13}C$	Long = -0.099 – 0.993; $\delta^{13}C$ = -5.708 – 52.160	1155.6 ± 34.0	0.0 ± 0.0	510.1 ± 22.6
BLK	~ Long + $\delta^{15}N$ + $(\delta^{15}N)^2$	7	509.4	0.3	0.1	Se ~ -1432.886 + 0.379 x Long + 227.300 x $\delta^{15}N$ - 8.376 x $(\delta^{15}N)^2$	Long = -0.199 – 0.951; $\delta^{15}N$ = 21.314 – 418.861; $(\delta^{15}N)^2$ = -15.745 – -0.522	1411 ± 37.6	0.0 ± 0.0	469 ± 21.7
	~ 1	4	509.5	0.4	0.1					
	~ $\delta^{13}C$	5	509.6	0.5	0.					
	~ $\delta^{15}N$	5	629.4	0	0.3	Se:Hg ~ 536.254 - 34.033 x $\delta^{15}N$	$\delta^{15}N$ = -53.387 – -14.176	2617 ± 51.2	0.0 ± 0.0	1038 ± 32.2
	~ Long + $\delta^{15}N$	6	630.8	1.4	0.2	Se:Hg ~ 526.060 + 0.354 x Long - 33.004 x $\delta^{15}N$	Long = -0.369 – 1.071; $\delta^{15}N$ = -51.840 – -12.539	2972 ± 54.5	0.0 ± 0.0	1055 ± 32.5
BG	~ $\delta^{15}N$ + $\delta^{13}C$	6	631.7	2.2	0.1					
	~ $\delta^{15}N$ + $(\delta^{15}N)^2$	6	631.9	2.4	0.1					
	~ Long * $\delta^{15}N$	7	631.9	2.5	0.1					
Blood Se :Hg	~ 1	4	644.9	0	0.3					
	~ Long	5	645.6	0.7	0.2					
BLK	~ Long : $\delta^{15}N$	5	645.9	1.0	0.2					
	~ $\delta^{15}N$	5	646.8	2.0	0.1					
	~ $\delta^{13}C$	5	646.9	2.0	0.1					

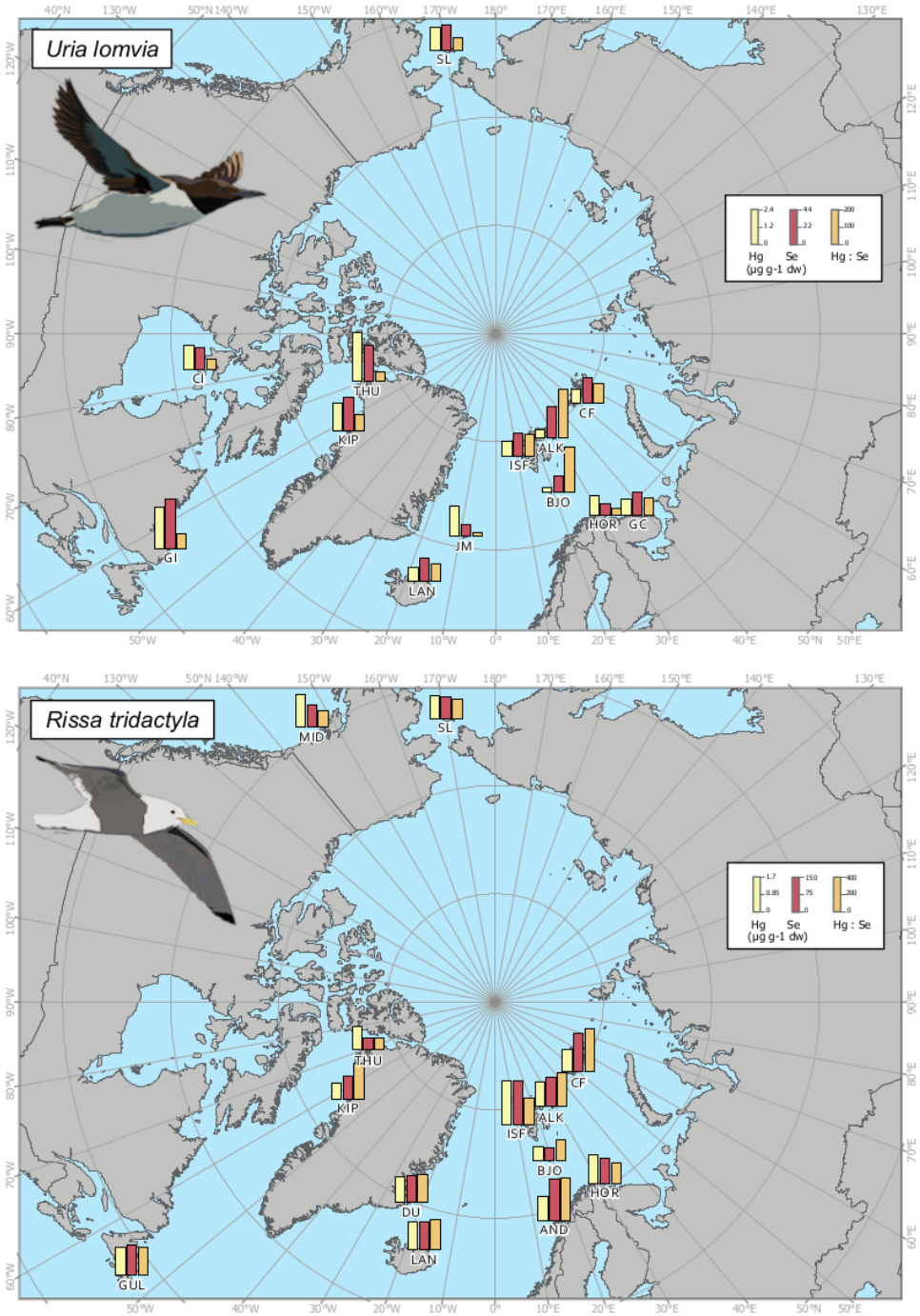

Figure 1. Distribution of Brünnich's guillemot (*Uria lomvia*) and black-legged kittiwake (*Rissa tridactyla*) colonies included in this study. Hg and Se concentrations (µg.g^{-1} dw), and Se:Hg ratios are shown in yellow, red and orange colours, respectively. Being the colony abbreviations (by ascending longitude degrees): SL for Saint Lawrence Is., MID for Middleton Is., CI for Coats Island, THU for Thule, KIP for Kippaku, GI for Gannets Island, GUL for Gull Island, DU for Dunholm; LAN for Langanes; JAN for Jan Mayen, AND for Anda, ISF for Isfjorden, ALK for Alkefjellet, BJO for Bjørnøya, HOR for Hornøya, GC for Gorodetski Cape, and CF for Cape Flora. Map conception: LIENSs - UMRi 7266. Credits: Made with Natural Earth. Free vector and raster map data @ naturalearthdata.com. PCS: North Pole Azimuthal Equidistant (epsg :102016). Brünnich guillemot and black-legged kittiwake drawings by courtesy of Julie Charrier.

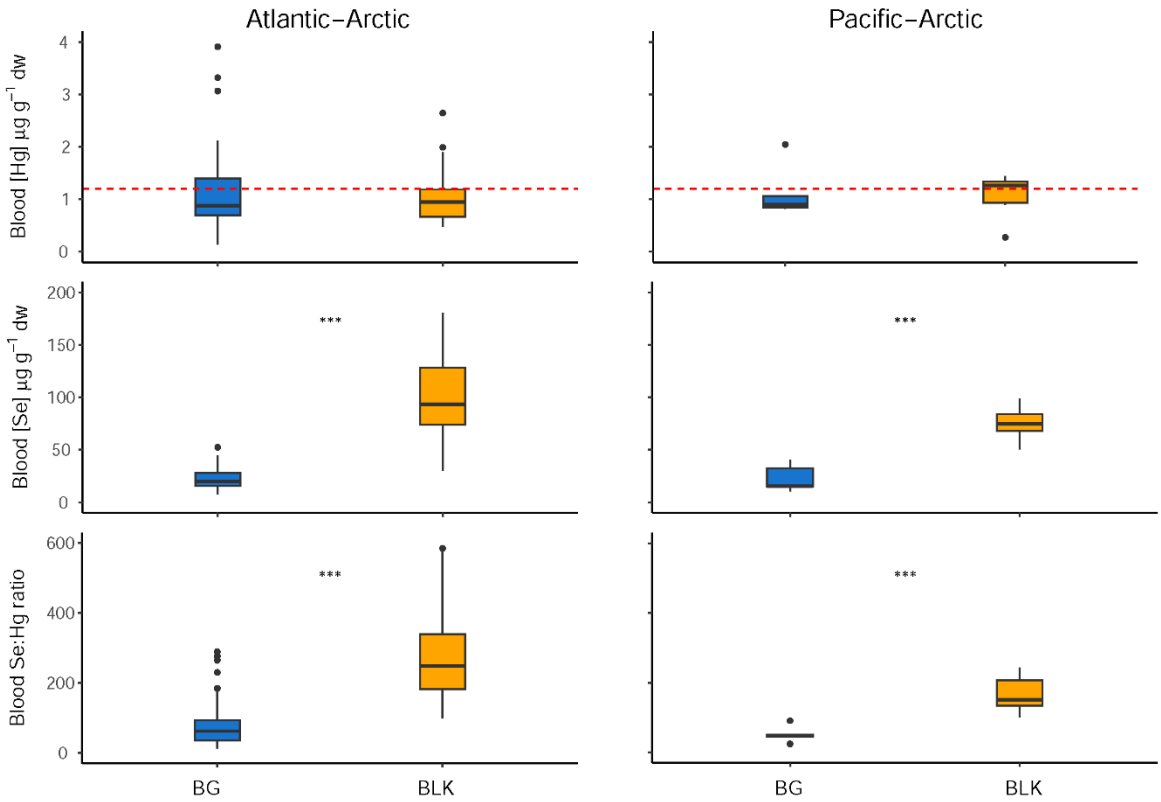

Figure 2. Boxplots of whole blood Hg and Se concentrations (µg.g^{-1} dw) and Se:Hg molar ratios by ocean basin (Atlantic-Arctic and Pacific-Arctic) and species: Brünnich's guillemots (*Uria lomvia*, BG; n= 60 for the Atlantic-Arctic and n= 5 for the Pacific-Arctic and all trace elements) and black-legged kittiwakes (*Rissa tridactyla*, BLK: n= 54, 53 and 52 for Hg, Se and Se:Hg in the Atlantic-Arctic; and n= 9, 8 and 8 in the Pacific). Significant differences between species per trace element and ocean, and calculated from linear mixed models, are shown with asterisks (*<0.5, **<0.01, ***<0.001). The red dashed line represents Hg concentrations from which eco-physiological impacts can be observed in birds (Ackerman et al. 2016).

Supplementary materials

Table S1. Mean (±SD) whole blood Hg, (µg.g^{-1} dw), Se:Hg ratio, δ^{15}N and δ^{13}C values (‰) in 13 populations of Brünnich's guillemot (BG; *Uria lomvia)* and 13 populations of black-legged kittiwakes (BLK; *Rissa tridactyla)* from the Artic and subarctic zone ordered by ascending longitude degrees. Ocean of belonging, longitude and latitude are specified. Significant differences between species obtained from Mann-Whitney tests are marked with bold numbers. Asterisk in the *p*-values denotes that the text could not compute exact *p*-value with ties.

				Hg		Se		Se:Hg		δ^{15}N		δ^{13}C	
	Long	**Lat**	**Years of sampling**	**BG**	**BLK**	**BG**	**BLK**	**BG**	**BLK**	**BG**	**BLK**	**BG**	**BLK**
Saint Lawrence (SL; USA)	-170.2	63.4	2016	1.13±0.52 n=5	0.87±0.43 n=4	22.71±13.12 n=5	74.23±24.37 n=3	51.7±24.3 n=5	183.4±74.4 n=3	17.3±0.4 n=5	15.9±1.42 n=4	-18.0±0.2 n=5	-18.5±0.2 n=4
				W = 9.5, *p*-value = 1*		W = 15, *p*-value = **0.036**		W = 15, *p*-value = **0.036**		W = 2, *p*-value = 0.063		W = 1, *p*-value = **0.032**	
Middleton (MID; USA)	-146.3	59.4	2016	-	1.28±0.21 n=5	-	76.59±9.13 n=5	-	155.3±30.8 n=5	-	14.9±0.2 n=5	-	-20.8±0.3 n=5
Coats Island (CI; Canada)	-83.1	62.5	2016	1.20±0.20 n=5	-	19.23±5.95 n=5	-	40.6±9.5 n=5	-	14.8±0.3 n=5	-	-20.3±0.1 n=5	-
Thule (THU; Greenland)	-69.2	77.5	2015	2.43±1.04 n=5	0.94±0.15 n=4	32.94±8.53 n=5	42.55±6.33 n=5	39.2±18.6 n=5	108.8±10.2 n=4	13.7±0.4 n=5	12.9±0.3 n=4	-20.2±0.1 n=5	-20.8±0.4 n=4
				W = 0, *p*-value = **0.016**		W = 20, *p*-value = 0.151		W = 20, *p*-value = **0.016**		$W_{1,7}$ = 0, *p*-value = **0.016**		W = 2, *p*-value = 0.063	
Kippaku (KIP; Greenland)	-56.6	73.7	BG: 2016 BLK: 2015	1.34±0.52 n=5	0.62±0.09 n=5	29.55±5.64 n=5	76.82±8.20 n=5	63.3±23.7 n=5	323.5±68.8 n=5	13.8±0.2 n=5	14.9±0.1 n=5	-20.0±0.1 n=5	-20.2±0.1 n=5
				W = 1, *p*-value **= 0.016**		$W_{1,8}$ = 25, *p*-value = **0.008**		W = 25, *p*-value = **0.008**		W = 3, *p*-value = 0.059		W = 3, *p*-value = 0.059*	
Gannets Island (GI; Canada)	-56.6	53.9	2015	2.04±0.74 n=5	-	43.94±9.50 n=5	-	61.9±26.1 n=5	-	13.9±0.3 n=5	-	-19.7±0.2 n=5	-
Gull Island (GUL; Canada)	-53.0	48.0	2017	-	1.09±0.35 n=5	-	104.30±35.45 n=5	-	253.9±71.6 n=5	-	12.2±0.6 n=5	-	-21.1±0.3 n=5
Dunholm (DU; Greenland)	-22.64	69.92	2017	-	1.00±0.32 n=5	-	93.91±6.65 n=5	-	261.5±92.8 n=5	-	14.2±0.2 n=5	-	-22.1±0.1 n=5
Langanes	-16.0	66.2	2016	0.72±0.11 n=5	1.1±0.53 n=5	20.75±3.28 n=5	97.92±30.42 n=5	73.3±7.4 n=5	271.3±171.2 n=5	11.8±0.1 n=5	12.1±0.5 n=5	-20.5±0.2 n=5	-20.7±0.2 n=5

(LAN; Iceland)				W = 19, *p*-value = 0.222	W = 25, *p*-value = **0.008**	W = 25, *p*-value = **0.008**	W = 17, *p*-value = 0.421	W = 3, *p*-value = 0.056
Jan Mayen (JM; Norway)	-8.3	71.0	2016	1.52±0.31 - n=5	10.75±2.70 - n=5	18.9±7.2 - n=5	12.2±0.2 - n=5	-22.0±0.1 - n=5
Anda (AND; Norway)	15.2	69.0	2017	- 0.95±0.35 n=5	- 141.62±33.06 n=5	- 392.7±66.7 n=5	- 12.3±0.3 n=5	- -20.5±0.1 n=5
Isfjorden (ISF; Norway)	15.5	78.3	2016	0.74±0.38 1.70±0.62 n=5 n=5 W = 25, *p*-value = **0.008**	20.09±4.50 148.72±19.08 n=5 n=5 W = 25, *p*-value = **0.008**	89.9±56.5 244.4±77.5 n=5 n=5 W = 24, *p*-value = **0.016**	13.0±0.6 12.2±0.6 n=5 n=5 W = 3, *p*-value = 0.056	-21.0±0.1 -20.9±0.2 n=5 n=5 W = 18.5, *p*-value = 0.249*
Alkefjellet (ALK; Norway)	18.5	79.6	2016	0.42±0.24 0.93±0.25 n=5 n=5 W = 24, *p*-value = **0.016**	27.89±6.25 99.68±19.24 n=5 n=5 W = 25, *p*-value = **0.008**	200.8±74.5 303.6±160.6 n=5 n=5 W = 18, *p*-value = 0.310	13.1±0.8 13.3±0.4 n=5 n=5 W = 16, *p*-value = 0.548	-20.8±0.3 -21.1±0.1 n=5 n=5 W = 3, *p*-value = 0.059*
Bjornoya (BJO; Norway)	19.0	74.5	2016	0.22±0.07 0.56±0.06 n=5 n=5 W = 25, *p*-value = **0.008**	14.80±3.14 42.19±11.87 n=5 n=3 W = 15, *p*-value = **0.036**	185.0±65.2 190.6±60.1 n=5 n=3 W = 9, *p*-value = 0.786	12.4±0.5 13.0±0.4 n=5 n=5 W = 21, *p*-value = 0.095	-21.1±0.1 -21.1±0.1 n=5 n=5 W = 12.5, *p*-value = 1*
Hornoya (HOR; Norway)	31.2	70.4	2016	0.94±0.12 1.13±0.30 n=5 n=5 W = 18, *p*-value = 0.310	10.21±2.75 85.24±36.55 n=5 n=5 W = 25, *p*-value = **0.008**	28.0±8.4 186.1±46.0 n=5 n=5 W = 25, *p*-value = **0.008**	14.3±0.3 14.2±0.3 n=5 n=5 W = 10, *p*-value = 0.691	-20.5±0.1 -20.5±0.2 n=5 n=5 W = 12, *p*-value = 1*
Gorodetski Cape (GC; Russia)	32.9	69.6	2015	0.77±0.04 - n=5	20.50±5.47 - n=5	67.9±18.4 - n=5	14.3±0.2 - n=5	-20.5±0.0 - n=5
Cape Flora (CF; Russia)	50.1	80.0	2016	0.71±0.11 0.88±0.16 n=5 n=5 W = 20.5, *p*-value = 0.116*	23.10±3.96 131.61±9.82 n=5 n=5 W = 25, *p*-value = **0.008**	83.6±14.5 390.2±86.6 n=5 n=5 W = 25, *p*-value = **0.008**	13.8±0.4 14.4±0.5 n=5 n=5 W = 22, *p*-value = 0.056	-21.8±0.5 -21.2±0.2 n=5 n=5 W = 25, *p*-value = **0.008**

Table S2. Modelling the spatial variation whole blood Hg, Se (µg.g^{-1} dw) and Se:Hg for Brünnich's guillemots (BG; *Uria lomvia*) and black-legged kittiwakes (BLK; *Rissa tridactyla*) from different colonies of the Atlantic-Arctic ocean. Colony and year were included as random factors. For each model we provide the number of parameters (K), the Akaike Information Criterion corrected for small sample size (AICc) value, and the ΔAICc value as the difference in AICc compared to the model with the lowest AICc value from its set of models (per trace element and species). From each set of models, we provide AICc values in ascending order. To reflect the effects of those factors from the best models (AICc lower than the null model and ΔAICc lower than two) we provide the regression functions and the confidence interval of their effects, as well as the variance ± SD of the random effects and the residuals.

								Random effects (Variance ± SD)		
	Model	**K**	**AICc**	**ΔAICc**	**Weight**	**Regression functions from the best model**	**Effect Confidence Interval (2.5 - 97.5%)**	**Colony**	**Year**	**Residual**
Blood Hg	~ Long + $\delta^{15}N$	6	100.2	0	0.2	Hg ~ -1.230 - 0.009 x Long + 0.173 x $\delta^{15}N$	Long = -0.017 – -0.003; $\delta^{15}N$ = -0.040 – 0.425	0.2 ± 0.4	0.1 ± 0.3	0.2 ± 0.4
	~ Long	5	100.2	0.0	0.2	Hg ~ -1.125 - 0.009 x Long	Long = -0.016 – -0.004	0.1 ± 0.3	0.2 ± 0.4	0.2 ± 0.4
	~ Long : $\delta^{15}N$	5	100.3	0.2	0.1					
	~ Long + $\delta^{13}C$ + $(\delta^{13}C)^2$	7	100.8	0.6	0.1	Hg ~ 115.616 - 0.008 x Long + 10.988 x $\delta^{13}C$ + 0.263 x $(\delta^{13}C)^2$	Long = -0.014 – -0.002; $\delta^{13}C$ = 0.000 – 23.946; $(\delta^{13}C)^2$ = 0.004 – 0.567	0.1 ± 0.3	0.2 ± 0.4	0.2 ± 0.4
	~ Long + $\delta^{15}N$ + $\delta^{13}C$ + $(\delta^{13}C)^2$	8	100.9	0.7	0.1					
	~ Long + $\delta^{15}N$ + $\delta^{13}C$	7	101.5	1.3	0.1					
	~ Long + $\delta^{13}C$	6	102.2	2.0	0.1					
	~ Long + $\delta^{15}N$ + $(\delta^{15}N)^2$	7	102.4	2.2	0.1					
	~ Long * $\delta^{15}N$	7	102.5	2.3	0.0					
	~ Lat + Long + $\delta^{15}N$ + $\delta^{13}C$	8	104.1	3.9	0.0					
	~ $\delta^{13}C$ + $(\delta^{13}C)^2$	6	104.4	4.3	0.0					
	~ $\delta^{15}N$ + $\delta^{13}C$ + $(\delta^{13}C)^2$	7	104.7	4.5	0.0					
	~ $\delta^{15}N$	5	105.0	4.9	0.0					
	~ $\delta^{15}N$ + $(\delta^{15}N)^2$	6	106.2	6.0	0.0					
	~ 1	4	106.8	6.6	0.0					
	$\delta^{15}N$ + $\delta^{13}C$	6	107.3	4.1	0.0					
	$\delta^{13}C$	5	107.8	7.6	0.0					
BG	Lat + $\delta^{15}N$ + $\delta^{13}C$	7	109.0	8.7	0.0					
BLK	~ $\delta^{15}N$ + $(\delta^{15}N)^2$	6	57.6	0	0.2	Hg ~ -20.975 + 3.226 x $\delta^{15}N$ - 0.118 x $(\delta^{15}N)^2$	$\delta^{15}N$ = 0.512 – 5.897; $(\delta^{15}N)^2$ = -0.220 – -0.016	0.1 ± 0.4	0.0 ± 0.0	0.1 ± 0.3

	~ d13C	5	58.3	0.7	0.2	Hg ~ 8.251 + 0.347 x $\delta^{13}C$	$\delta^{13}C$ = -0.054 – 0.750	0.1 ± 0.4	0.0 ± 0.0	0.1 ± 0.3
	~ 1	4	58.5	0.9	0.1					
	~ $\delta^{15}N$ + $\delta^{13}C$	6	59.1	1.5	0.1					
	~ $\delta^{13}C$ + $(\delta^{13}C)^2$	6	59.9	2.3	0.1					
	~ $\delta^{15}N$	5	60.1	2.5	0.1					
	~ Long + $\delta^{15}N$ + $(\delta^{15}N)^2$	7	60.2	2.6	0.1					
	~ Long + $\delta^{13}C$	6	60.4	2.8	0.1					
	~ Long : $\delta^{15}N$	5	60.7	3.1	0.0					
	~ Long	5	60.7	3.1	0.0					
	~ Lat + $\delta^{15}N$ + $\delta^{13}C$	7	61.4	3.8	0.0					
	~ Long + $\delta^{15}N$ + $\delta^{13}C$	7	61.6	4.0	0.0					
	~ Long + $\delta^{15}N$	6	62.6	4.9	0.0					
	~ Lat + Long + $\delta^{15}N$ + $\delta^{13}C$	8	63.6	6.0	0.0					
	~ Long * $\delta^{15}N$	7	65.2	7.6	0.0					
BG	~ Long	5	414.8	0	0.2	Se ~ 23.995 - 0.084 x Long	Long = -0.212 – 0.015	52.0 ± 7.2	43.8 ± 6.6	30.9 ± 5.6
	~ Long : $\delta^{15}N$	5	415.3	0.5	0.2	Se ~ 24.160 - 0.005 x Long : $\delta^{15}N$	Long: $\delta^{15}N$ = -0.014 – 0.001	52.0 ± 7.2	47.2 ± 6.9	31.1 ± 5.6
	~ 1	4	415.4	0.5	0.2					
	~ δ13C	5	416.5	1.6	0.1					
	~ Long * $\delta^{15}N$	7	416.9	2.0	0.1					
	~ Long + $\delta^{13}C$	6	417.0	2.1	0.1					
	~ Long + $\delta^{15}N$	6	417.2	2.4	0.1					
	~ $\delta^{15}N$	5	417.6	2.8	0.1					
	~ $\delta^{13}C$ + $(\delta^{13}C)^2$	6	418.1	3.2	0.0					
	~ $\delta^{15}N$ + $\delta^{13}C$	6	419.0	4.1	0.0					
	~ Long + $\delta^{15}N$ + $\delta^{13}C$	7	419.5	4.7	0.0					
	~ Long + $\delta^{15}N$ + $(\delta^{15}N)^2$	7	419.7	4.9	0.0					
	~ $\delta^{15}N$ + $(\delta^{15}N)^2$	6	420.0	5.2	0.0					
	~ Lat + $\delta^{15}N$ + $\delta^{13}C$	7	421.4	6.6	0.0					
	~ Lat + Long + $\delta^{15}N$ + $\delta^{13}C$	8	422.1	7.3	0.0					
BLK	~ Long	5	509.1	0	0.1	Se ~ 99.567 + 0.421 x Long	Long = -0.083 – 0.923	943.2 ± 30.7	0.0 ± 0.0	552.0 ± 23.5
	~ Long + $\delta^{13}C$	6	509.3	0.1	0.1	Se ~ 617.064 + 0.455 x Long + 24.730 x $\delta^{13}C$	Long = -0.099 – 0.993; $\delta^{13}C$ = -5.708 – 52.160	1155.6 ± 33.99	0.0 ± 0.0	510.1 ± 22.6

Blood Se

	~ Long + $\delta^{15}N$ + $(\delta^{15}N)^2$	7	509.4	0.3	0.1	Se ~ -1432.886 + 0.379 x Long + 227.300 x $\delta^{15}N$ - 8.376 x $(\delta^{15}N)^2$	Long = -0.199 – 0.951; $\delta^{15}N$ = 21.314 – 418.861; $(\delta^{15}N)^2$ = -15.745 – -0.522	1411 ± 37.6	0.0 ± 0.0	469 ± 21.7
	~ 1	4	509.5	0.4	0.1					
	~ $\delta^{13}C$	5	509.6	0.5	0.1					
	~ Long:$\delta^{15}N$	5	509.7	0.6	0.1					
	~ $\delta^{15}N$	5	510.5	1.4	0.1					
	~ Long * $\delta^{15}N$	7	510.6	1.5	0.1					
	~ Long + $\delta^{15}N$	6	510.9	1.8	0.1					
	~ $\delta^{15}N$ + $\delta^{13}C$	6	511.2	2.0	0.0					
	~ Long + $\delta^{15}N$ + $\delta^{13}C$	7	511.4	2.3	0.0					
	~ Lat + Long + $\delta^{15}N$ + $\delta^{13}C$	8	512.8	3.6	0.0					
	~ Lat + $\delta^{15}N$ + $\delta^{13}C$	7	513.8	4.6	0.0					
Blood Se :Hg	~ $\delta^{15}N$	5	629.4	0	0.3	Se:Hg ~ 536.254 - 34.033 x $\delta^{15}N$	$\delta^{15}N$ = -53.387 – -14.176	2617 ± 51.2	0.0 ± 0.0	1038 ± 32.2
	~ Long + $\delta^{15}N$	6	630.8	1.4	0.2	Se:Hg ~ 526.060 + 0.354 x Long - 33.004 x $\delta^{15}N$	Long = -0.369 – 1.071; $\delta^{15}N$ = -51.840 – -12.539	2972 ± 54.5	0.0 ± 0.0	1055 ± 32.5
BG	~ $\delta^{15}N$ + $\delta^{13}C$	6	631.7	2.2	0.1					
	~ $\delta^{15}N$ + $(\delta^{15}N)^2$	6	631.9	2.4	0.1					
	~ Long * $\delta^{15}N$	7	631.9	2.5	0.1					
	~ Lat + Long + $\delta^{15}N$ + $\delta^{13}C$	7	632.2	2.9	0.1					
	~ Lat + $\delta^{15}N$ + $\delta^{13}C$	7	632.4	3.0	0.1					
	~ Long + $\delta^{15}N$ + $(\delta^{15}N)^2$	7	633.4	3.9	0.0					
	~ Lat + Long + $\delta^{15}N$ + $\delta^{13}C$	8	634.0	4.6	0.0					
	~ 1	4	638.0	8.6	0.0					
	~ $\delta^{13}C$ + $(\delta^{13}C)^2$	6	638.1	8.7	0.0					
	~ Long	5	638.4	9.0	0.0					
	~ Long : $\delta^{15}N$	5	638.6	9.2	0.0					
	~ $\delta^{13}C$	5	639.3	9.9	0.0					
	~ Long + $\delta^{13}C$	6	640.7	11.3	0.0					
	~ 1	4	644.9	0	0.3					
BLK	~ Long	5	645.6	0.7	0.2	Se:Hg ~ 273.035 - 0.812 x Long	Long = -0.464 – 2.089	4817 ± 69.41	0.0 ± 0.0	9345 ± 96.67
	~ Long : $\delta^{15}N$	5	645.9	1.0	0.2	Se:Hg ~ 272.343 - 0.055 x Long : $\delta^{15}N$	Long : $\delta^{15}N$ = -0.040 – 0.149	4934 ± 70.24	0.0 ± 0.0	9363 ± 96.76

~ $\delta^{15}N$	5	646.8	2.0	0.1	Se:Hg ~ 529.100 – 19.760 x $\delta^{15}N$	$\delta^{15}N$ = -68.370 – 27.221	6817 ± 82.57	0.0 ± 0.0	8998 ± 94.86
~ $\delta^{13}C$	5	646.9	2.0	0.1					
~ Long + $\delta^{15}N$	6	647.7	2.8	0.1					
~ Long + $\delta^{13}C$	6	647.9	3.1	0.1					
~ Long * $\delta^{15}N$	7	648.6	3.7	0.0					
~ $\delta^{15}N$ + $\delta^{13}C$	6	649.0	4.1	0.0					
~ Long + $\delta^{15}N$ + $(\delta^{15}N)^2$	7	649.7	4.8	0.0					
~ Long + $\delta^{15}N$ + $\delta^{13}C$ +	7	650.2	5.3	0.0					
~ Lat + $\delta^{15}N$ + $\delta^{13}C$	7	651.5	6.7	0.0					
~ Lat + Long + $\delta^{15}N$ + $\delta^{13}C$	8	652.9	8.0	0.0					

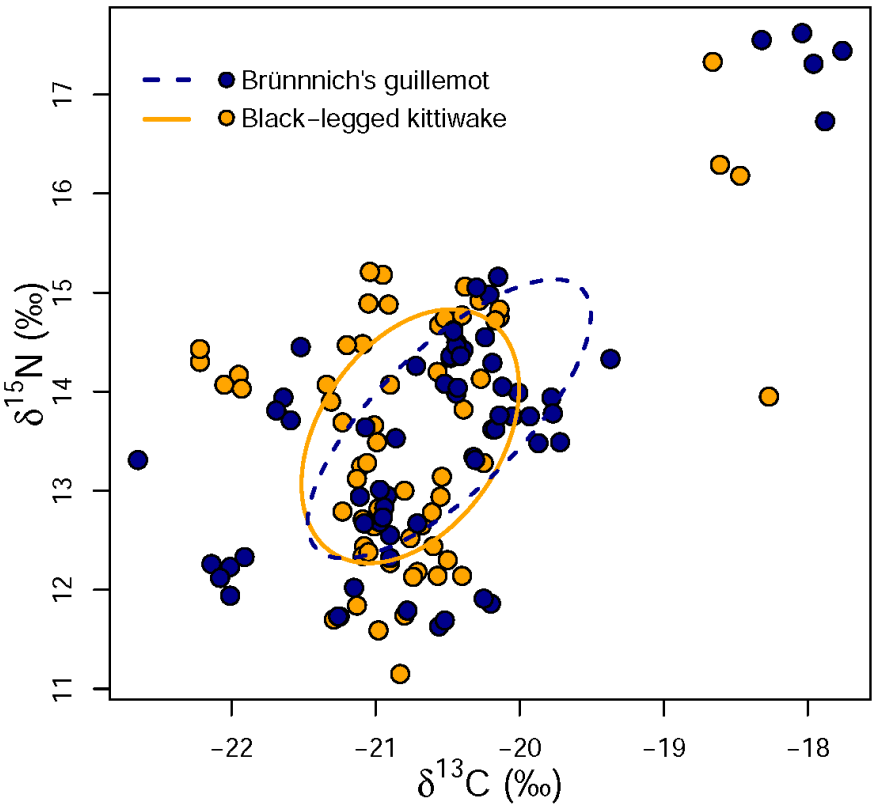

Figure S1. Biplots of blood $\delta^{15}N$ and $\delta^{13}C$ values and Standard Bayesian Ellipses for Brünnich's guillemot (*Uria lomvia*, blue colours and dashed lines) and black-legged kittiwake (*Rissa tridactyla*, in orange colours and continuous lines).

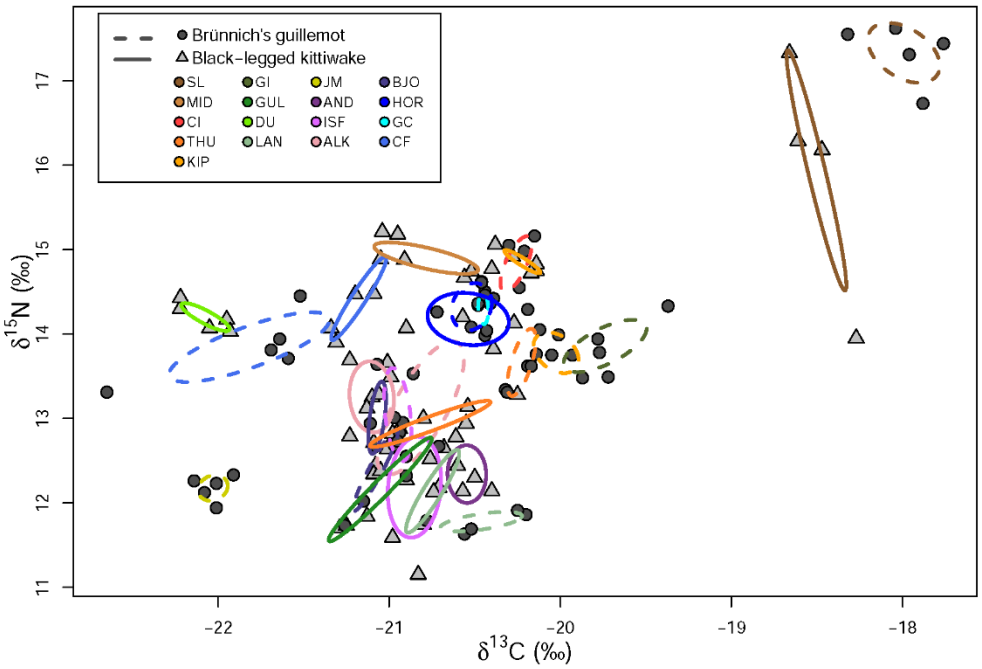

Figure S2. Biplots of blood $\delta^{15}N$ and $\delta^{13}C$ values and Standard Bayesian Ellipses for Brünnich's guillemot (*Uria lomvia*, dark grey circles and dashed lines) and Black-legged kittiwake (*Rissa tridactyla*, grey triangles and continuous lines). The different colours of the Standard Bayesian Ellipses correspond to different colonies, being the colony abbreviations (by ascending longitude degrees): SL for Saint Lawrence Is., MID for Middleton Is., CI for Coats Island, THU for Thule, KIP for Kippaku, GI for Gannets Island, GUL for Gull Island, DU for Dunholm; LAN for Langanes; JAN for Jan Mayen, AND for Anda, ISF for Isfjorden, ALK for Alkefjellet, BJO for Bjørnøya, HOR for Hornøya, GC for Gorodetski Cape, and CF for Cape Flora.